UNCLASSIFIED

AD 133160

Armed Services Technical Information Agency

Reproduced by

DOCUMENT SERVICE CENTER

KNOTT BUILDING, DAYTON, 2, OHIO

UNCLASSIFIED

NAVORD REPORT 4259

HEAT—TRANSFER CHARACTERISTICS OF A HEMISPHERE CYLINDER AT HYPERSONIC MACH NUMBERS

FC

11 APRIL 1957

U. S. NAVAL ORDNANCE LABORATORY
WHITE OAK, MARYLAND

NAVORD Report 4259

Aeroballistic Research Report 336

HEAT-TRANSFER CHARACTERISTICS OF A HEMISPHERE CYLINDER AT HYPERSONIC MACH NUMBERS

Prepared by:

E. M. Winkler
and
J. E. Danberg

ABSTRACT: The heat-transfer characteristics of the laminar compressible boundary layer on a hemisphere cylinder have been investigated at free-stream Mach numbers of 5, 6.5, and 8. The Reynolds number based on free-stream conditions and model diameter was varied from 70,000 to 700,000. Various conditions of steady-state heat transfer to the model were realized by circulating a coolant through the model, and by varying the tunnel supply air temperature. The wall to stagnation temperature ratio was varied from 0.43 to 0.75. Optical observations and Pitot pressure surveys of the boundary layer showed it to be laminar on both the hemisphere and the cylindrical afterbody. The heat transfer was evaluated from the temperature differences measured across the model wall under steady-state conditions. Over the hemisphere, the local non-dimensional heat-transfer parameters are, on the average, approximately twenty percent larger than predicted for an isothermal body by Korobkin's modified incompressible theory.

U. S. NAVAL ORDNANCE LABORATORY
WHITE OAK, MARYLAND

NAVORD Report 4259

This report is an account of the hemisphere cylinder heat-transfer program carried out in the NOL 12 x 12 cm Hypersonic Tunnel No. 4.

Knowledge of the heat-transfer characteristics of blunt-nosed bodies has become of particular interest. The blunt nose alleviates some of the design difficulties resulting from the high rates of heat transfer and low heat capacity near the nose of pointed bodies.

A portion of the results contained in this NAVORD Report was presented at the 24th Annual Meeting of the Institute of Aeronautical Sciences in January 1956. The present report contains additional results and a more detailed analysis of the data as well as a complete tabulation of the experimental results.

This work was jointly sponsored by the U. S. Naval Bureau of Ordnance and the U. S. Air Force. It was carried out under Tasks NOL-133-1-56, and NOL-291.

The authors wish to express their indebtedness to Drs. R. E. Wilson, R. K. Lobb and Mr. I. Korobkin for many stimulating discussions during the course of the investigations. A large portion of the numerical evaluation was done by Mr. Moon H Cha. Mr. R. Garren, Jr., in addition to participating in the tests, was largely responsible for the model design and test preparations.

WILLIAM W. WILBOURNE
Captain, USN
Commander

H. H. KURZWEG
By direction

CONTENTS

ILLUSTRATIONS

SYMBOLS

C_p	pressure coefficient
D	model diameter
h	heat-transfer coefficient
k	thermal conductivity of air
k_m	thermal conductivity of model material
M	Mach number
Nu	Nusselt number
p	static pressure
Pr	Prandtl number
Re	Reynolds number
Δr	wall thickness of model
T	temperature
ΔT	temperature difference across wall
T_o	stagnation temperature
T_{eff}	effective temperature (surface temperature for zero heat transfer)
u	velocity
x	model contour length, measured from stagnation point
Δy	effective model wall thickness, defined by Equations 3 and 4
α	angular position, measured from stagnation point
β	velocity gradient at stagnation point
μ	absolute viscosity of air
ν	kinematic viscosity
ρ	density of air

Subscripts

D	diameter used as characteristic length
e	adiabatic wall conditions
L	local conditions at outer edge of model boundary layer
w	conditions at or on model wall
x	contour length used as characteristic length
∞	free-stream conditions at infinity

HEAT-TRANSFER CHARACTERISTICS OF A HEMISPHERE CYLINDER AT HYPERSONIC MACH NUMBERS

INTRODUCTION

1. When the present investigations were initiated, experimental information on the heat-transfer characteristics of laminar compressible boundary layers on blunt-nosed bodies were still rather limited inspite of the great practical interest in such body shapes. Most of the available data were obtained at Mach numbers below 5, and for small rates of heat transfer (references a-c). In each of these investigations attempts were made to simulate isothermal bodies. For these data, incompressible and modified compressible theories represent the over-all trend.

2. In order to realize larger rates of heat transfer, and to perform the investigations at hypersonic Mach numbers, the present studies were carried out on a cooled hemisphere cylinder in the NOL Hypersonic Tunnel No. 4 (reference d), at Mach numbers 5, 6.5, and 8. Free-stream Reynolds numbers based on model diameter ranged from 7×10^4 to 7.7×10^5, and the model wall to stagnation temperature ratios from 0.43 to 0.75.

Description of Models and Experimental Procedure

3. The pressure and heat-transfer models are 3.8 cm diameter hemisphere cylinders made of type 302 stainless steel. They have a constant wall thickness, and can be cooled or heated internally to temperatures ranging from 210°K to 800°K. Pressure data were obtained at 10 positions along the hemispherical nose and the cylindrical afterbody with the pressure model shown in Figure 1. The pressure orifices, arranged in a spiral starting at the stagnation point, are 0.635 mm in diameter, which corresponds to an angle of 1.9 degrees on the model, or to an arc length, $\Delta x/D$, of 0.0167. Mercury manometers or oil manometers which have reading accuracies of ± 0.1 mm Hg and ± 0.001 mm Hg, respectively, were used to measure the pressures. A reference pressure orifice is located in both the pressure and the heat-transfer model at $x/D = 0.869$.

4. The heat-transfer model, shown partially assembled in Figure 2, has thermocouples located at 11 stations on both

the exterior and interior wall.* Type 302 stainless steel was selected for the models because its thermal conductivity varies linearily with temperature over the entire range considered for the tests. Also, the coefficient of thermal conductivity of this material is sufficiently small to assure a fair accuracy in measuring temperature differences across the model wall.

5. The coolant (silicon oil DC 200, 2 centistoke) enters the model through a tube which is concentric to the cylinder, and is then discharged into the hemisphere nose. The coolant returns through the annular clearance between the inlet tube and the model wall. The main entrance and exit passages of the coolant are part of the model support. The cooling system requirements were calculated by equaling the heat transfer from the air to the model to that from the model to the coolant. This is done by assuming the following: (1) the major contribution to the over-all heat transfer is due to the heat transfer to the hemispherical nose of the model; (2) the distribution of the latter can be predicted by the theory of reference (a); and (3) the absolute value at the stagnation point can be taken as the mean value of the experimental data reported in reference (a). From this procedure, together with the available engineering data for the silicon oil, a circulation rate of 4 gallons/minute was computed if the bulk temperature rise of the coolant should remain smaller or equal to 1°C for all test conditions. The measured temperature rise for this flow rate was well within the predicted limit, except at the lowest coolant temperature (about 210°K) where it amounted to 3°C. An exterior, thermostatically controlled temperature bath maintained the coolant at any desired temperature within the range from 210°K to 370°K. For higher temperatures, hot air was circulated through the model at a rate that its temperature rise or drop between entrance and exit was negligible.

6. The interior thermocouples are made of 30-gauge iron

---

*A first model provided for 3 thermocouples at each of the 11 stations. The model wall thickness was calculated, using the results of reference(a), to vary from the stagnation point to the shoulder in such a fashion that for a constant interior temperature also a constant exterior temperature should have been obtained. The thermocouples were then placed on calculated isothermes in the model wall. Preliminary test results did not verify that the thermocouples were located on isothermes.

The model described above has a simpler construction which alleviated some of the difficulties in the assembly but has the disadvantage of providing for only 2 readings at each station.

constantan Ceramo wires.* The exterior thermocouples, located radially above each interior one, are made of 36-gauge iron constantan wires and are imbedded in grooves on the model surface with an insulating cement.** The sizes of the grooves, of the thermocouple junctions, and of the spherical recesses into which the interior junctions are welded, are such that the thermocouples are located with an accuracy better than ± 0.025 cm. To reduce the conduction losses along the exterios thermocouple wires, the grooves into which the wires are imbedded form at least a semi-circle around the model and then they lead the wires straight back to the base of the afterbody. The exterior and interior temperatures were recorded on two synchronized operating 12-point Brown recorders which have printing intervals of two seconds. Temperature readings, accurate to ± 0.1°C, were taken after practically steady-state conditions were reached, which required 5 to 10 minutes operation at the desired test conditions.

7. In addition to the pressure and temperature distributions, measurements were also made of the surface temperatures for zero heat transfer. For these tests hot air was circulated through the model and the temperature adjusted until a locally zero temperature gradient was observed successively for each station.

8. Information on the flow pattern and the condition of the boundary layer around the model was obtained from schlieren observations and boundary-layer surveys.

Data Reduction

9. The free-stream conditions were determined from measurements of the wall static and Pitot pressures in the test section, and from recordings of the stagnation temperature, T_O, in the nozzle inlet. The Rayleigh formula was used to compute the Mach number. The local flow conditions around the model, in terms of M_L, T_L, ρ_L, and u_L were calculated from the measured pressure distributions and T_O. In making these calculations, the flow was assumed to expand isentropically over the model, and the stagnation point pressure was set equal to the Pitot pressure. The boundary-layer surveys indicated that these assumptions are justified.

---

*Manufactured by Thermo Electric Co., Inc., Fair Lawn, New Jersey.

**Technical B copper cement, manufactured by W. V-B Ames Co., Fremont, Ohio

10. Other relations and quantities used in the further evaluation of the data are the pressure coefficient

$$c_p = (p_L - p_\infty)/(\tfrac{1}{2})(\rho_\infty u_\infty^2) \qquad (1)$$

The Nusselt number based on either the model diameter or the arc length are:

$$Nu_D = \frac{hD}{k} = \frac{qD}{(T_e - T_w)k_{air}} \quad ; \quad Nu_x = \frac{hx}{k} = \frac{qx}{(T_e - T_w)k_{air}} \qquad (2)$$

The heat transferred from the air to the model, q, is calculated from the heat conducted through the model shell where the contribution of radiation heat transferred to or from the model is neglected. The heat transfer, q, is equal to the average conductivity, k_m, of model material multiplied by the temperature gradient at the model surface (reference 1). Assuming one-dimensional conduction, that is neglecting the transverse conduction along the body contour, the temperature gradient at the model surface is (reference 1),

$$\frac{\Delta T}{\Delta y} = \frac{\Delta T}{D\Delta r} \quad (D - 2\Delta r) \qquad (3)$$

for the hemisphere,

$$\frac{\Delta T}{\Delta y} = \frac{2\Delta T}{D \log_e \frac{D}{(D-2\Delta r)}} \qquad (4)$$

for the cylinder. The adiabatic wall temperature T_e for a laminar boundary layer is

$$T_e = (Pr)^{1/2}(T_o - T_L) + T_L \qquad (5)$$

Consistent with the usual representations of heat-transfer data, the Nusselt numbers are ratioed to either $(\beta D^2/\nu)^{1/2}$ or $Re_x^{1/2}$ where β is the velocity gradient at the stagnation point

$$\beta = \left(\frac{du_L}{dx}\right)_{\alpha = 0} \qquad (6)$$

and

$$Rex = \frac{u_L x}{\nu} \tag{7}$$

For the viscosity of air Sutherland's formula was used (NBS Table 2.39). The thermal conductivity of air was obtained using the empirical formula

$$k = \frac{0.6325 \times 10^{-5} T^{3/2}}{T + 245.4 \times 10^{-12/T}} \text{ cal/cm sec } ^{o}C \tag{8}$$

(NBS Table 2.42). Prandtl number values were taken from the NBS Table 2.44. The thermal conductivity of the 302 stainless steel was measured on a sample cut from the model stock by the National Bureau of Standards (reference f).

11. In addition to computing the heat-transfer coefficient on the basis of (T_e-T_w), experimental values of the surface temperature for locally zero heat transfer, T_{eff}, have also been used instead of T_e. In general, the measured T_{eff} data are not free from radiation losses, since the tunnel walls are, in some cases, cooler than the model by a factor of 2.5. These data were therefore corrected assuming a cylindrical geometry of tunnel and model, and an emissivity of 0.7.

RESULTS

Pressure Measurements

12. The Mach number distributions obtained from the pressure measurements over the model are shown in Figure 3. The distribution over the hemisphere is consistent with the results of references (a-c). Over the cylindrical afterbody the Mach number continues to rise slowly approaching a value which appears to depend on the free-stream Mach number.

13. The measured pressure distributions presented as pressure coefficients are shown in Figure 4. The absolute values of the pressure coefficient for the forward half of the hemisphere are lower than Newtonian theory predicts, but are closely represented by a curve calculated using Pitot pressure to determine C_{pmax}. The agreement is good for small values of x/D, but the experimental C_p data deviate from the calculated $\cos^2 2\, x/D$ curve at values of x/D larger than about 0.5. Near this point,

for the Mach number range 5 to 8, the pressure distribution has the same slope as one assuming a Prandtl-Meyer expansion and good agreement with the data is obtained if the Prandtl-Meyer calculation is started at the point of equal slopes.

14. The velocity gradient at the stagnation point used in correlating the heat-transfer data was determined from graphs of the velocity distribution over the hemisphere. The local velocity was calculated from the measured pressure distribution and the stagnation temperature. Values of the normalized velocity gradient, $\beta D/u_{\infty}$, are plotted in Figure 5. Values obtained from the experimental Mach number distributions are compared with the data of references (a, b, c, h, i, j, and k) and with a theoretical curve based on the Newtonian pressure distribution. The present velocity gradients are about 10 percent higher than theory predicts.

Boundary-Layer Surveys

15. The boundary layer was surveyed at 5 stations along the model at a free-stream Mach number, M_{∞}, of 8. For these tests, hot air was circulated through the model at the temperature necessary to achieve practically zero heat transfer at the stagnation point. Pitot probes of a half-height of 0.005 inch were used for the surveys. To evaluate the Mach number distribution across the boundary layer, the measured Pitot pressures were referred to the local wall-static pressure value. The surveys shown in Figure 6 are characteristic of laminar boundary layers. A slight overshoot was measured beyond the juncture of the hemisphere and the cylinder $x/D = 0.869$, which is probably due to an over-expansion at the juncture. For each station, the Mach number at the outer edge of the boundary layer agrees closely with the Mach number, M_L, obtained from the ratio of the local wall-static pressure and the pressure measured at the stagnation point. A comparison of these data with theory was felt not to be justified because their further evaluation would require measured distributions of the boundary-layer temperature which were not obtained during the present investigations.

16. For the free-stream Mach numbers 6.5 and 5, schlieren optical observations were made which also confirmed a laminar boundary layer for the entire model.

Heat-Transfer Measurements

17. The measured temperature distributions deviate considerably from an isothermal wall. For small rates of heat

transfer, the temperature varied from 330°K at the stagnation point to 304°K at the shoulder (see Appendix A $M_\infty =$ 5.11). For higher rates of heat transfer a variation from 368°K to 266°K was observed (Appendix A $M_\infty = 4.9$). Because the inside wall temperature remained relatively constant in all cases, the non-isothermal surface temperature distributions are reflected in the relative temperature differences which are shown in Figure 7.

18. The calculation of surface heat transfer from the measured temperature differences was based on the assumption of one-dimensional heat flow across the model wall. The deviation from an isothermal temperature distribution shows this is only a first approximation. An attempt was made to obtain a better approximation by evaluating the effect of the conduction along the model. The principal procedure tried assumos no conductivity variation and uses the solution of Laplace's equation in spherical coordinates with flow axis symmetry with the inside and outside temperature distributions as the boundary conditions. This procedure did not give consistant results, mainly because the number of measurements were insufficient tó define the derivatives of the distribution on which the longitudinal conduction depends.

19. The over-all behavior of the curves of Figure 7 differs at two places from the distribution predicted by incompressible theory. The temperature difference has a maximum at $x/D = 0.0975$ ($\alpha \sim 11°$), and not at $\alpha = 0$. An increased temperature difference occurs, in some cases quite pronounced, at $x/D = 0.393$ ($\alpha = 45°$) which corresponds approximately to the intersection of the sonic line with the body contour. Measurements in addition to those presented in Figure 7 showed that the maximum off the stagnation point decreases with decreasing rate of heat transfer and disappears for the case of zero heat transfer. Recently published data (reference h, Figure 10) obtained by the transient technique indicates the temperature distribution develops a maximum approximately 4 1/2 degrees from the stagnation point as steady-state conditions are approached.

20. The heat-transfer data, expressed as $Nu_x/(Re_x)^{1/2}$, are shown in Figures 8a through 8h. The numerical values for all 34 surveys are given in the tables. The tabulated values of $Nu_x/(Re_x)^{1/2}$ are based on T_w and T_e. For the graphical representations, the reference temperatures T_w and T_{eff} have been used. The conversion quantity $(T_e-T_w)/(T_{eff}-T_w)$ is included in the tables.

DISCUSSION OF DATA

21. In general, the plots of the non-dimensional heat-transfer

parameters exhibit, in either representation, the behavior already indicated in Figure 7. For each heat-transfer condition and Mach number, the individual distributions show a rather characteristic behavior which repeats itself, more or less, with variation in free-stream Reynolds number. Some characteristic features are, however, clearly shown by all distributions, the peaks at $x/D = 0.0975$ ($\alpha \sim 11^{o}$) and at $x/D = 0.393$ ($\alpha = 45^{o}$), as well as the rather large values of the parameter at the shoulder. It is difficult to draw any conclusions regarding a trend with either Mach number, Reynolds number or heat-transfer rate. The band representing all the data is considerably wider than can be explained by experimental scatter, which is of the order of $\pm$ 5 percent.

22. The effect of reference temperature (at which the properties of air are evaluated) is illustrated in Figure 9. While the selection of wall temperature or temperature at the outer edge of the model boundary layer as reference temperature has very little effect, not more than about 1.5 percent for the T_w and T_L values encountered, the use of T_{eff} instead of T_e has the tendency to flatten the distributions.

23. In Figure 10a and 10b are shown the present data, together with other experimental results, and with theory. The latter has been done only to orient the present data with reference to theoretical predictions which are based on the concept of an isothermal body and one-dimensional heat conduction. In comparison to Silbulkin's stagnation point value of 0.661 (reference g) all data are high. All experimental data exhibit the same general behavior over the front portion of the hemisphere. The stagnation point value is not a maximum value. (The Crawford and McCauley data, reference h, show a similar effect near the stagnation point as their test approaches steady-state conditions.) Like the present results, Stine and Wanlass' data show a peak value at $\alpha \sim 11^{o}$, and another one at $\alpha = 45^{o}$, and 60^{o}, respectively. Beyond this point, Stine and Wanlass' data decrease rapidly and approach the flat plate value. Not so the present data, the behavior of which is consistent with Gruenewald and Fleming's and Korobkin's results. The numerical values are, on the average, 20 percent larger than predicted by Korobkin's modified incompressible theory.

24. Finally, in Figure 11, the local Stanton number values computed from the data obtained up to about 75^{o} angular position are compared with $St = 0.763\ Pr^{-0.6}\ Re_x^{-0.5}$ (reference a). Though the experimental data exhibit the same slope as the above relation, the numerical values are, on the average, about 12.5 percent larger.

CONCLUDING REMARKS

25. The heat-transfer characteristics of a hemisphere-cylinder have been investigated at hypersonic Mach numbers from 5 to $M = 8$, and model wall to stagnation temperature ratios from 0.43 to 0.75. The data have been evaluated from temperature difference measurements made across the wall on a cooled model after practically steady-state conditions were reached.

26. The distributions of the pressure coefficient ratio $C_p/C_{p\,max}$ over the hemisphere follow the $\cos^2$-law on the forward part of the hemisphere. Near the shoulder they agree with those calculated by assuming a Prandtl-Meyer expansion.

27. The wall temperature difference distributions exhibit a maximum at the 11-degree angular position. This maximum was found to disappear for the case of zero heat transfer.

28. The distributions of the local non-dimensional heat-transfer parameter show peak values for angular positions of about 11 degrees and 45 degrees, and high values at the shoulder.

29. The numerical results are about 20 percent larger than calculated for an isothermal body by the modified incompressible theory, given by Korobkin.

REFERENCES

(a) Korobkin, Irving, "Laminar Heat-Transfer Characteristics of a Hemisphere for the Mach Number Range 1.9 to 4.9," NAVORD Report 3841, October 1954

(b) Gruenewald, K. H., and Fleming, W. J., "Laminar Heat Transfer to a Hemisphere at Mach Number 3.2," NAVORD Report 3980, February 1956

(c) Stine, H. A., and Wanlass, K., "Theoretical and Experimental Investigation of Aerodynamic Heating and Isothermal Heat-Transfer Parameters on a Hemispherical Nose with Laminar Boundary Layer at Supersonic Mach Numbers," NACA TN 3344, December 1954

(d) Wegener, P., Lobb, R. K., Winkler, E. M., Sibulkin, M., and Staab, H., "NOL Hypersonic Tunnel No. 4 Results V: Experimental and Theoretical Investigation of a Cooled Hypersonic Wedge Nozzle," NAVORD Report 2701, April 1953

(e) Richards, L. E., and Robinson, H. E., "Thermal Conductivity of a Specimen of Stainless Steel Type 302," NBS Report 4132, June 1955

(f) Lees, L., Hypersonic Flow, Paper presented at the Fifth International Aeronautical Conference, June 20-24, 1955, Preprint No. 554

(g) Sibulkin, M., "Heat Transfer Near the Forward Stagnation Point of a Body of Revolution," J. Aero. Sci., 19, 570, 1952

(h) Crawford, D. H., and McCauley, W. D., "Investigation of the Laminar Aerodynamic Heat-Transfer Characteristics of a Hemisphere-Cylinder in the Langley 11-Inch Hypersonic Tunnel at a Mach Number of 6.8," NACA TN 3706, March 1956

(i) Oliver, R. E., "An Experimental Investigation of Flow Over Simple Blunt Bodies at a Nominal Mach Number of 5.8," GALCIT Hypersonic Wind Tunnel Memo, No. 26, June 1955

(j) Stalder, J. R., and Nielsen, H. V., "Heat Transfer from a Hemisphere-Cylinder Equipped with Flow Separation Spikes," NACA TN 3287, September 1954

(k) Korobkin, I., "Local Flow Conditions, Recovery Factors and Heat Transfer Coefficients on the Nose of a Hemisphere-Cylinder at a Mach Number of 2.8," NAVORD Report 2865, May 1953

(1) Schneider, P. J., "Conduction Heat Transfer," Addison-Wesley Publishing Co., Pg. 7 and 14, 1955

$M_\infty = 5.11$ $T_o = 461^oK$ $Re_{D\infty} = 1.15 \times 10^5$ $p_o = 2.14$ ATM

$[(T_e - T_w)/T_e]_m = .28$ $\beta D/U_\infty = 1.22$ $U_\infty = 889$ M/sec

x/D	$p/p_{\alpha=0}$	T_w °K	ΔT °K	$(T_e-T_w)/(T_{eff}-T_w)$	Nu_x	$Nu_x/\sqrt{Re_x}$
0	1.0000	333	29.4	1.024	0	.928**
.098		335	31.0	1.030	56.0	.997
.164		330	26.0	1.021	69.3	.853
.257		326	23.2*	1.008	97.0	.789
.302	.652					
.393		323	20.5	1.030	137	.956
.424	.437					
.518		313	15.0*	1.012	131	.887
.547	.243					
.658		307	7.2	1.043	84.3	.661
.720	.0953					
.785		304	4.8	1.083	66.5/85.6	.621/.801
.805	.0669					
.869		303	3.9	1.088	77.9	.735
.898	.0610					
1.652	.0566					
1.848		302*	2.5*	1.003	105	.720
2.320	.0577					
2.848		301	1.1	1.000	71.2	.399
2.985	.0495					

$M_\infty = 5.00$ $T_o = 469^oK$ $Re_{D\infty} = 4.04 \times 10^5$ $p_o = 6.56$ ATM

$[(T_e - T_w)/T_e]_m = .249$ $\beta D/U_\infty = 1.24$ $U_\infty = 886$ M/sec

x/D	$p/p_{\alpha=0}$	T_w °K	ΔT °K	$(T_e-T_w)/(T_{eff}-T_w)$	Nu_x	$Nu_x/\sqrt{Re_x}$
0	1.0000	357	43.5	1.028	0	.863**
.098		359	44.5	1.021	78.7	.951
.164		353	38.0	1.018	111	.799
.257		348	33.5*	1.012	154	.775
.302	.645					
.393		342	31.5	1.016	222	.858
.424	.507					
.518		328	21.5*	1.038	197	.858
.547	.237					
.658		319	12.5	1.047	149	.652
.720	.0826					
.785		314	8.5	1.043	125/157	.734/.743
.805	.0567					
.869		312	7.0	1.043	144	.743
.898	.0472					
1.652	.0387					
1.848		310*	5.0*	1.008	219	.617
2.320	.0332					
2.848		308	3.0	1.000	207	.415
2.985	.0288					

$M_\infty = 4.99$ $T_o = 462^oK$ $Re_{D\infty} = 2.30 \times 10^5$ $p_o = 4.03$ ATM

$[(T_e - T_w)/T_e]_m = .261$ $\beta D/U_\infty = 1.23$ $U_\infty = 879$ M/sec

x/D	$p/p_{\alpha=0}$	T_w °K	ΔT °K	$(T_e-T_w)/(T_{eff}-T_w)$	Nu_x	$Nu_x/\sqrt{Re_x}$
0	1.0000	345	33.2	1.031	0	.799**
.098		349	35.6	1.028	62.3	.913
.164		341	29.4	1.017	79.8	.700
.257		337	27.6*	1.013	122	.752
.302	.648					
.393		332	26.7	1.009	193	.959
.424	.439					
.518		319	16.5*	1.039	150	.725
.547	.241					
.658		311	9.7	1.044	107	.663
.720	.0856					
.785		307	6.7	1.053	98.7/122	.593/.732
.805	.0559					
.869		306	5.6	1.085	114	.827
.898	.0497					
1.652	.0425					
1.848		304*	3.7*	1.012	160	.862
2.320	.0.12					
2.848		302	1.8	1.000	119	.535
2.985	.0365					

*Temperature interpolation

**$Nu_D/(\beta D^2/\nu)^{1/2}$

$M_\infty = 5.02$ $T_o = 450^oK$ $Re_{D\infty} = 5.61 \times 10^5$ $p_o = 9.86$ ATM

$[(T_e - T_w)/T_e]_m = .224$ $\beta D/U_\infty = 1.23$ $U_\infty = 869$ M/sec

x/D	$p/p_{\alpha=0}$	T_w °K	ΔT °K	$(T_e-T_w)/(T_{eff}-T_w)$	Nu_x	$Nu_x/\sqrt{Re_x}$
0	1.0000	355	42.7	1.035	0	.939**
.098		358	43.0	1.025	91.3	.931
.164		352	36.9	1.019	126	.828
.257		348	33.7*	1.015	182	.821
.302	.643					
.393		342	31.4	1.019	265	.911
.424	.445					
.518		328	22.5*	1.042	242	.770
.547	.237					
.658		319	12.4	1.054	176	.596
.720	.0817					
.785		314	8.0	1.049	140/192	.546/.749
.805	.0502					
.869		312	6.4	1.049	153	.597
.898	.0495***					
1.652	.0386					
1.848		310*	4.2	1.008	214	.605
2.320	.0347					
2.848		308	2.9	1.000	228	.550
2.985	.0360					

* Temperature interpolation

** $Nu_D/(\beta D^2/\nu)^{1/2}$

*** Pressure interpolation

$M_\infty = 5.01$
$T_o = 423^oK$
$Re_{D\infty} = 7.68 \times 10^5$
$P_o = 12.0$ ATM

$[(T_e - T_w)/T_e]_m = .169$
$\beta D/U_\infty = 1.27$
$U_\infty = 844$ M/sec

x/D	$p/p_{\alpha=0}$	$T_w{}^oK$	ΔT^oK	$(T_e-T_w)/(T_{eff}-T_w)$	Nu_x	$Nu_x/\sqrt{Re_x}$
0	1.0000	350	37.4	1.023	0	.927**
.098		353	38.7	1.025	109	1.029
.164		348	33.5	1.023	151	.875
.257		344	30.8*	1.042	219	.872
.302	.647					
.393		338	27.8	1.075	309	.941
.424	.445					
.518		325	19.7*	1.152	274	.768
.547	.236					
.658		317	9.9	1.172	181	.546
.720	.0801					
.785		312	6.4	1.180	148/183	.514/.636
.805	.0496					
.869		311	4.8	1.161	153	.519
.898	.0507					
1.652	.0460					
1.848		309*	3.4*	1.131	228	.561
2.320	.0327					
2.848		308	2.0	1.160	247	.540
2.985	.0298					

$M_\infty = 4.93$
$T_o = 560^oK$
$Re_{D\infty} = 1.36 \times 10^5$
$P_o = 3.17$ ATM

$[(T_e - T_w)/T_e]_m = .453$
$\beta D/U_\infty = 1.21$
$U_\infty = 967$ M/sec

x/D	$p/p_{\alpha=0}$	$T_w{}^oK$	ΔT^oK	$(T_e-T_w)/(T_{eff}-T_w)$	Nu_x	$Nu_x/\sqrt{Re_x}$
0	1.0000	345	94.6	1.008	0	1.257**
.098		350	83.6	1.003	75.9	1.189
.164		338	62.9	1.000	93.7	.879
.257		330	58.0*	.996	135	.857
.302	.656					
.393		320	54.2	1.020	194	.977
.424	.449					
.518		292	41.5*	1.032	190	.887
.547	.248					
.658		271	24.3	1.006	144	.753
.720	.0927					
.785		257	27.7	1.040	195/241	1.190/1.467
.805	.0600					
.869		252	20.9	1.061	201	1.238
.898	.0532					
1.652	.0422					
1.848		245*	13.0*	1.005	247	1.277
2.320	.0337					
2.848		238	5.0	.986	159	.672
2.985	.0312					

$M_\infty = 5.09$
$T_o = 575^oK$
$Re_{D\infty} = .705 \times 10^5$
$P_o = 1.87$ ATM

$[(T_e - T_w)/T_e]_m = .485$
$\beta D/U_\infty = 1.20$
$U_\infty = 985$ M/sec

x/D	$p/p_{\alpha=0}$	$T_w{}^oK$	ΔT^oK	$(T_e-T_w)/(T_{eff}-T_w)$	Nu_x	$Nu_x/\sqrt{Re_x}$
0	1.000	328	82.7	1.008	0	1.293**
.098		332	73.1	1.002	58.4	1.196
.164		321	54.5	1.000	72.5	.890
.257		312	51.0*	.996	106	.883
.302	.658					
.393		305	47.7	1.012	156	1.036
.424	.446					
.518		279	31.0*	1.031	132	.804
.547	.247					
.658		261	19.5	1.005	107	.716
.720	.102					
.785		249	22.9	1.044	150/185	1.164/1.384
.805	.0693					
.869		245	16.7	1.060	150	1.166
.898	.0621					
1.652	.0566					
1.848		241*	12.6*	1.019	241	1.350
2.320	.0529					
2.848		238	8.5	.999	252	1.174
2.985	.0465					

* Temperature interpolation
** $Nu_D/(\beta D^2/\nu)^{1/2}$

$M_\infty = 4.90$
$T_o = 571^oK$
$Re_{D\infty} = 1.88 \times 10^5$
$P_o = 3.79$ ATM

$[(T_e - T_w)/T_e]_m = .434$
$\beta D/U_\infty = 1.22$
$U_\infty = 975$ M/sec

x/D	$p/p_{\alpha=0}$	$T_w{}^oK$	ΔT^oK	$(T_e-T_w)/(T_{eff}-T_w)$	Nu_x	$Nu_x/\sqrt{Re_x}$
0	1.0000	368	115	1.009	0	1.478**
.098		375	93.4	1.003	87.9	1.319
.164		362	75.9	1.000	117	1.047
.257		354	71.0*	0.995	170	1.034
.302	.652					
.393		341	66.5	1.012	242	1.157
.424	.446					
.518		308	51.0*	1.030	233	1.027
.547	.246					
.658		283	30.5	0.996	178	.869
.720	.0920					
.785		266	33.3	1.040	228/282	1.288/1.597
.805	.0593					
.869		261	25.3	1.054	237	1.355
.898	.0538					
1.652	.0406					
1.848		253*	15.5*	.996	313	1.417
2.320	.0325					
2.848		245	5.9	.982	183	.723
2.985	.0298					

* Temperature interpolation
** $Nu_D/(\beta D^2/\nu)^{1/2}$

$M_\infty = 6.56$, $T_o = 548^oK$, $Re_{D\infty} = 1.52 \times 10^5$, $P_o = 6.7$ ATM
$[(T_e - T_w)/T_e]_m = .269$, $\beta D/U_\infty = 1.265$, $U_\infty = 995$ M/sec

x/D	$p/p_{\alpha=0}$	T_w °K	ΔT °K	$(T_e-T_w)/(T_{eff}-T_w)$	Nu_x	$Nu_x/\sqrt{Re_x}$
0	1.000	393	28.9	1.013	0	.702**
.098		394	29.0	1.000	35.8	.736
.164		390	26.7	1.000	55.1	.694
.257		386	24.8*	1.000	81.4	.724
.302	.627					
.393		381	20.0	1.018	105	.775
.424	.390					
.518		374	13.9*	1.067	100	.742
.547	.211					
.658		368	8.6	1.169	83.1	.750
.720	.0911					
.785		364	6.6	1.189	79.2/97.5	.911/1.12
.805	.0477					
.869		363	6.0	1.170	100	1.19
.898	.0425					
1.652	.0330					
1.848		361*	3.6*	1.045	130	1.29
2.320	.0263					
2.848		362	3.0	1.000	173	1.62
2.985	0224					

$M_\infty = 6.58$, $T_o = 548^oK$, $Re_{D\infty} = 2.51 \times 10^5$, $P_o = 11.25$ ATM
$[(T_e - T_w)/T_e]_m = .260$, $\beta D/U_\infty = 1.263$, $U_\infty = 995$ M/sec

x/D	$p/p_{\alpha=0}$	T_w °K	ΔT °K	$(T_e-T_w)/(T_{eff}-T_w)$	Nu_x	$Nu_x/\sqrt{Re_x}$
0	1.000	402	35.7	1.014	0	.730**
.098		403	35.0	1.006	45.7	.753
.164		398	33.0	1.000	71.2	.717
.257		394	30.0*	1.003	102	.725
.302	.626					
.393		389	25.5	1.022	140	.874
.424	.400					
.518		379	17.5*	1.061	130	.777
.547	.211					
.658		371	10.0	1.175	98.4	.705
.720	.0775					
.785		367	7.5	1.142	92.1/113	.842/1.040
.805	.0467					
.869		366	6.5	1.164	110	1.030
.898	.0415					
1.652	.0304					
1.848		362*	3.7*	1.054	135	1.049
2.320	.0235					
2.848		364	3.0	1.008	176	1.286
2.985	.0186					

$M_\infty = 6.58$, $T_o = 548^oK$, $Re_{D\infty} = 2.08 \times 10^5$, $P_o = 9.35$ ATM
$[(T_e - T_w)/T_e]_m = .263$, $\beta D/U_\infty = 1.263$, $U_\infty = 995$ M/sec

x/D	$p/p_{\alpha=0}$	T_w °K	ΔT °K	$(T_e-T_w)/(T_{eff}-T_w)$	Nu_x	$Nu_x/\sqrt{Re_x}$
0	1.000	399	34.5	1.014	0	.756**
.098		401	34.3	1.006	43.8	.785
.164		396	32.0	1.003	68.2	.749
.257		392	29.5*	1.003	100	.775
.302	.627					
.393		387	24.5	1.024	132	.838
.424	.399					
.518		377	16.5*	1.060	121	.784
.547	.215					
.658		369	9.7	1.172	94.2	.735
.720	.0788					
.785		365	7.5	1.139	91.0/108	.910/1.077
.805	.0474					
.869		364	6.5	1.171	108	1.11
.898	.0422					
1.652	.0305					
1.848		361*	4.4*	1.053	159	1.35
2.320	.0228					
2.848		363	3.2	1.004	186	1.49
2.985	.0186					

* Temperature interpolation
** $Nu_D/(\beta D^2/\nu)^{1/2}$

$M_\infty = 6.57$, $T_o = 548^oK$, $Re_{D\infty} = 2.96 \times 10^5$, $P_o = 13.23$ ATM
$[(T_e - T_w)/T_e]_m = .252$, $\beta D/U_\infty = 1.266$, $U_\infty = 993$ M/sec

x/D	$p/p_{\alpha=0}$	T_w °K	ΔT °K	$(T_e-T_w)/(T_{eff}-T_w)$	Nu_x	$Nu_x/\sqrt{Re_x}$
0	1.000	408	39.7	1.014	0	.782**
.098		410	39.3	1.000	53.2	.817
.164		404	36.5	1.000	79.8	.748
.257		401	33.7*	1.000	119	.796
.302	.627					
.393		394	27.6	1.020	155	.842
.424	.401					
.518		383	18.5*	1.071	142	.776
.547	.212					
.658		374	11.3	1.018	114	.755
.720	.0759					
.785		370	7.5	1.260	94.2/117	.793/.981
.805	.0460					
.869		370	6.9	1.179	120	1.04
.898	.0410					
1.652	.0304					
1.848		365*	4.8*	1.046	180	1.30
2.320	.0235					
2.848		365	2.7	1.000	159	1.08
2.985	.0186					

* Temperature interpolation
** $Nu_D/(\beta D^2/\nu)^{1/2}$

M_∞ = 6.49 $[(T_e-T_w)/T_e]_m$ = .407
T_o = 606°K $\beta D/U_\infty$ = 1.25
$Re_{D\infty}$ = 1.51 x 10^5 U_∞ = 1045 M/sec
p_o = 7.38 ATM

x/D	$p/p_{\alpha=0}$	T_w °K	ΔT°K	$(T_e-T_w)/(T_{eff}-T_w)$	Nu_x	$Nu_x/\sqrt{Re_x}$
0	1.0000	369	54.4	1.009	0	.763**
.098		370	53.5	1.000	43.4	.774
.164		364	49.5	1.004	67.0	.735
.257		358	45.5*	1.004	97.1	.737
.302	.631					
.393		352	39.4	1.039	131	.816
.424	.395					
.518		332	23.0*	1.057	103	.619
.547	.218					
.658		323	15.5	1.048	90.5	.643
.720	.0860					
.785		317	12.3	1.059	88.3/109	.780/.962
.805	.0499					
.869		314	8.8	1.068	86.5	.693
.898	.0454					
1.652	.0322					
1.848		309*	5.5*	1.013	115	.861
2.320	.0261					
2.848		307	2.1	.983	67.4	.462
2.985	.0219					

M_∞ = 6.50 $[(T_e-T_w)/T_e]_m$ = .40
T_o = 606°K $\beta D/U_\infty$ = 1.26
$Re_{D\infty}$ = 1.95 x 10^5 U_∞ = 1045 M/sec
p_o = 9.52 ATM

x/D	$p/p_{\alpha=0}$	T_w °K	ΔT°K	$(T_e-T_w)/(T_{eff}-T_w)$	Nu_x	$Nu_x/\sqrt{Re_x}$
0	1.000	374	57.5	1.009	0	.727**
.098		376	57.5	1.000	47.2	.737
.164		370	53.9	1.009	74.0	.701
.257		364	50.0*	1.009	108	.679
.302	.635					
.393		357	43.4	1.040	102	.814
.424	.399					
.518		335	25.0*	1.048	111	.603
.547	.212					
.658		326	17.6	1.049	103	.645
.720	.0830					
.785		319	13.4	1.060	96.3/119	.752/.928
.805	.0494					
.869		315	9.8	1.069	96.3	.783
.898	.0449					
1.652	.0324					
1.848		310*	6.1*	1.013	129	.850
2.320	.0259					
2.848		308	2.4	.987	79.0	.479
2.985	.0217					

* Temperature interpolation
** $Nu_D/(\beta D^2/\nu)^{1/2}$

M_∞ = 6.48 $[(T_e-T_w)/T_e]_m$ = .39
T_o = 602°K $\beta D/U_\infty$ = 1.22
$Re_{D\infty}$ = 2.37 x 10^5 U_∞ = 1040 M/sec
p_o = 11.57 ATM

x/D	$p/p_{\alpha=0}$	T_w °K	ΔT°K	$(T_e-T_w)/(T_{eff}-T_w)$	Nu_x	$Nu_x/\sqrt{Re_x}$
0	1.000	378	61.4	1.005	0	.740**
.098		383	63.7	.958	54.7	.801
.164		375	58.9	1.004	83.7	.750
.257		368	53.3*	1.004	119	.742
.302	.637					
.393		360	46.8	1.020	163	.834
.424	.402					
.518		343*	27.6*	1.045	162	.806
.547	.214					
.658		328	19.5	1.052	116	.668
.720	.0806					
.785		320	14.8	1.054	108	.764
.805	.0495					
.869		316	11.0	1.057	110	.808
.898	.0451					
1.652	.0329					
1.848		312*	6.5*	1.023	139	.835
2.320	.0267					
2.848		307	2.9	.995	96	.525
2.985	.0220					

M_∞ = 6.41 $[(T_e-T_w)/T_e]_m$ = .395
T_o = 607°K $\beta D/U_\infty$ = 1.28
$Re_{D\infty}$ = 2.97 x 10^5 U_∞ = 1042 M/sec
p_o = 14.5 ATM

x/D	$p/p_{\alpha=0}$	T_w °K	ΔT°K	$(T_e-T_w)/(T_{eff}-T_w)$	Nu_x	$Nu_x/\sqrt{Re_x}$
0	1.000	387	68.4	1.009	0	.718**
.098		389	69.4	1.005	59.2	.740
.164		382	64.2	1.005	91.7	.709
.257		376	59.7*	1.005	135	.739
.302	.640					
.393		367	52.1	1.023	183	.823
.424	.405					
.518		345	35.0*	1.044	125	.683
.547	.218					
.658		331	22.1	1.055	125	.663
.720	.825					
.785		322	17.2	1.075	123	.774
.805	.0497					
.869		318	12.9	1.079	127	.816
.898	.0451					
1.652	.0328					
1.848		313*	8.3*	1.022	175	.920
2.320	.0261					
2.848		309	3.6	1.004	117	.528
2.985	.0219					

* Temperature interpolation
** $Nu_D/(\beta D^2/\nu)^{1/2}$

M_∞ = 6.58 $[(T_e-T_w)/T_e]_m$ = .51
T_o = 660°K $\beta D/U_\infty$ = 1.268
$Re_{D\infty}$ = 1.84 x 10^5 U_∞ = 1091 M/sec
P_o = 11.2 ATM

x/D	$p/p_{\alpha=0}$	ΔT_w °K	T°K	$(T_e-T_w)/(T_{eff}-T_w)$	Nu_x	$Nu_x/\sqrt{Re_x}$
0	1.000	369	72.5	1.010	0	.658**
.098		370	76.8	1.007	49.7	.724
.164		358	80.5	.997	88.3	.776
.257		346	76.0*	1.000	126	.760
.302	.627					
.393		330	65.9	1.017	170	.824
.424	.396					
.518		300	48.5*	1.019	163	.755
.547	.211					
.658		277	32.0	1.034	140	.730
.720	.0777					
.785		264	31.6	1.034	153/188	.992/1.22
.805	.0450					
.869		264	31.9	1.049	212	1.41
.898	.0405					
1.652	.0318					
1.848		247*	19.5*	1.017	299	1.52
2.320	.0238					
2.848		237	6.8	1.000	163	.756
2.985	.0198					

M_∞ = 6.55 $[(T_e-T_w)/T_e]_m$ = .48
T_o = 660°K $\beta D/U_\infty$ = 1.265
$Re_{D\infty}$ = 2.95 x 10^5 U_∞ = 1095 M/sec
P_o = 17.2 ATM

x/D	$p/p_{\alpha=0}$	T_w °K	ΔT °K	$(T_e-T_w)/(T_{eff}-T_w)$	Nu_x	$Nu_x/\sqrt{Re_x}$
0	1.000	393	84.8	1.011	0	.688**
.098		395	91.6	1.004	61.5	.761
.164		379	94.0	.996	105	.774
.257		364	88.0*	1.000	152	.765
.302	.630					
.393		346	75.3	1.017	210	.807
.424	.401					
.518		315	55.0*	1.020	190	.735
.547	.211					
.656		289	38.6	1.035	171	.738
.720	.0774					
.785		272	35.5	1.038	190/233	1.015/1.246
.805	.0441					
.869		271	34.5	1.055	251	1.076
.898	.0407					
1.652	.0323					
1.848		257*	21.3*	1.018	380	1.548
2.320	.0241					
2.848		243	8.9	1.000	213	.802
2.985	.0201					

M_∞ = 6.55 $[(T_e-T_w)/T_e]_m$ = .51
T_o = 660°K $\beta D/U_\infty$ = 1.256
$Re_{D\infty}$ = 2.35 x 10^5 U_∞ = 1093 M/sec
P_o = 14.13 ATM

x/D	$p/p_{\alpha=0}$	T_w °K	ΔT °K	$(T_e-T_w)/(T_{eff}-T_w)$	Nu_x	$Nu_x/\sqrt{Re_x}$
0	1.000	387	82.4	1.011	0	.712**
.098		389	87.9	1.004	59.3	.768
.164		372	89.6	1.003	98.4	.777
.257		358	74.1*	1.000	143	.786
.302	.627					
.393		341	72.8	1.017	203	.837
.424	.398					
.518		302	53.3*	1.019	183	.736
.547	.212					
.658		285	36.5	1.035	163	.773
.720	.0749					
.785		269	34.5	1.038	184/226	1.088/1.337
.805	.0456					
.869		269	34.7	1.054	256	1.550
.898	.0406					
1.652	.0314					
1.848		247*	18.0*	1.017	278	1.139
2.320	.0243					
2.848		241	8.1	1.000	197	.797
2.985	.0201					

* Temperature interpolation
** $Nu_D/(\beta D^2/\nu)^{1/2}$

M_∞ = 6.58 $[(T_e-T_w)/T_e]_m$ = .47
T_o = 653°K $\beta D/U_\infty$ = 1.275
$Re_{D\infty}$ = 3.61 x 10^5 U_∞ = 1085 M/sec
P_o = 21.25 ATM

x/D	$p/p_{\alpha=0}$	T_w °K	ΔT °K	$(T_e-T_w)/(T_{eff}-T_w)$	Nu_x	$Nu_x/\sqrt{Re_x}$
0	1.000	398	85.4	1.012	0	.665**
.098		402	93.7	1.002	68.1	.774
.164		385	96.7	1.008	112	.764
.257		370	92.0*	1.004	172	.805
.302	.637					
.393		351	78.3	1.011	216	.808
.424	.398					
.518		321	59.0*	1.003	217	.775
.547	.211					
.658		292	38.7	1.013	179	.716
.720	.0782					
.785		273	36.0	1.010	202/248	101/121
.805	.0472					
.869		272	35.0	1.026	262	1.29
.898	.0435					
1.652	.0325					
1.848		252*	22.0*	1.019	365	1.34
2.320	.0255					
2.848		244	8.2	.966	211	.797
2.985	.0215					

* Temperature interpolation
** $Nu_D/(\beta D^2/\nu)^{1/2}$

M_∞ = 8.01
T_o = 645°K
$Re_{D\infty}$ = 1.58 x 10^5
P_o = 15.00 ATM

$[(T_e-T_w)/T_e]_m$ = .362
$\beta D/U_\infty$ = 1.18
U_∞ = 1105 M/sec

x/D	$p/p_{\alpha=0}$	T_w°K	ΔT°K	$(T_e-T_w)/(T_{eff}-T_w)$	Nu_x	$Nu_x/\sqrt{Re_x}$
0	1.000	420	46.5	1.018	0	.731**
.098		425	51.3	1.011	38.3	.790
.164		414	41.8	1.002	57.4	.716
.257		408	37.5*	1.003	81.2	.716
.302	.639					
.393		402	34.5	1.028	117	.869
.424	.409					
.518		387	22.2*	1.035	100	.740
.547	.208					
.658		376	13.3	1.030	79.0	.681
.720	.0826					
.785		372	9.8	1.004	72.0/88.6	.739/.909
.805	.0566					
.869		369	7.3	1.000	73.6	.785
.898	.0480					
1.652	.0346					
1.848		367*	5.5*	1.000	119	1.006
2.320	.0371					
2.848		363	1.8	1.021	58.9	.389
2.985	.0371					

M_∞ = 7.99
T_o = 643°K
$Re_{D\infty}$ = 2.45 x 10^5
P_o = 22.9 ATM

$[(T_e-T_w)/T_e]_m$ = .377
$\beta D/U_\infty$ = 1.19
U_∞ = 1094 M/sec

x/D	$p/p_{\alpha=0}$	T_w°K	ΔT°K	$(T_e-T_w)/(T_{eff}-T_w)$	Nu_x	$Nu_x/\sqrt{Re_x}$
0	1.000	426	48.5	1.019	0	.713**
.098		432	55.0	1.013	46.7	.867
.164		424	48.5	1.005	69.6	.780
.257		416	43.5*	1.006	97.7	.757
.302	.647					
.393		408	38.2	1.029	135	.859
.424	.414					
.518		393	25.0*	1.034	118	.738
.547	.219					
.658		381	15.8	**1.029**	**97.2**	**.721**
.720	.0808					
.785		375	11.0	1.000	82.5/102	.648/.796
.805	.0514					
.869		373	9.2	.993	95.8	.926
.898	.0421					
1.652	.0278					
1.848		366*	3.3*	.984	73.7	.609
2.320	.0249					
2.848		365	1.5	1.000	51.0	.329
2.985	.0307					

M_∞ = 8.00
T_o = 645°K
$Re_{D\infty}$ = 1.80 x 10^5
P_o = 20.9 ATM

$[(T_e-T_w)/T_e]_m$ = .360
$\beta D/U_\infty$ = 1.20
U_∞ = 1095 M/sec

x/D	$p/p_{\alpha=0}$	T_w°K	ΔT°K	$(T_e-T_w)/(T_{eff}-T_w)$	Nu_x	$Nu_x/\sqrt{Re_x}$
0	1.000	424	49.4	1.018	0	.809**
.098		429	54.9	1.014	46.4	.965
.164		418	45.4	1.004	63.1	.786
.257		411	40.5*	1.006	88.0	.758
.302	.637					
.393		404	36.2	1.031	124	.871
.424	.414					
.518		389	24.0*	1.033	110	.774
.547	.215					
.658		378	14.8	**1.023**	**89.0**	**.735**
.720	.0810					
.785		372	10.2	.998	75.3/92.9	.762/.939
.805	.0533					
.869		372	9.7	.995	99.0	1.05
.898	.0435					
1.652	.0298					
1.848		365*	3.1*	.991	69.0	.610
2.320	.0302					
2.848		362	0.5	1.009	16.5	.106
2.985	.0380					

* Temperature interpolation
** $Nu_D/(\beta D^2/\nu)^{1/2}$

M_∞ = 7.99
T_o = 641°K
$Re_{D\infty}$ = 3.11 x 10^5
P_o = 28.90 ATM

$[(T_e-T_w)/T_e]_m$ = .345
$\beta D/U_\infty$ = 1.195
U_∞ = 1091 M/sec

x/D	$p/p_{\alpha=0}$	T_w°K	ΔT°K	$(T_e-T_w)/(T_{eff}-T_w)$	Nu_x	$Nu_x/\sqrt{Re_x}$
0	1.000	431	51.9	1.014	0	.716**
.098		436	58.0	1.010	51.9	.848
.164		429	51.8	1.003	76.2	.767
.257		422	48.2*	1.005	111	.773
.302	.634					
.393		413	42.3	1.030	153	.875
.424	.413					
.518		397	28.5*	1.032	137	.775
.547	.227					
.658		383	18.3	**1.029**	**114**	**.745**
.720	.0864					
.785		376	12.0	.993	92.0/113	.741/.912
.805	.0506					
.869		374	10.2	.988	108	.930
.898	.0421					
1.652	.0275					
1.848		367*	3.5*	.978	79.1	.593
2.320	.0212					
2.848		365	1.8	.993	62.2	.370
2.985	.0253					

* Temperature interpolation
** $Nu_D/(\beta D^2/\nu)^{1/2}$

$M_\infty = 8.00$
$T_o = 664.5°K$
$Re_{D\infty} = .913 \times 10^5$
$p_o = 9.15$ ATM

$[(T_e-T_w)/T_e]_m = .462$
$\rho U/U_\infty = 1.193$
$U_\infty = 1113$ M/sec

x/D	$p/p_{\alpha=0}$	T_w °K	ΔT°K	$(T_e-T_w)/(T_{eff}-T_w)$	Nu_x	$Nu_x/\sqrt{Re_x}$
0	1.000	376.5	57.5	1.007	0	.975**
.098		377	56.7	1.010	38.7	.964
.164		365	46.0	1.000	51.5	.777
.257		357.5	41.0*	1.003	72.0	.765
.302	.646					
.393		351	38.0	1.011	105	.910
.424	.421					
.518		334	24.5*	1.024	89.7	.755
.547	.220					
.658		321.5	14.5	1.013	71.2	.688
.720	.0955					
.785		316.5	12.0	1.018	69.5/65.4	.759/.970
.805	.0648					
.869		321	16.8	1.013	124	1.43
.898	.0588					
1.652	.0486					
1.848		313.5*	10.0*	1.013	169	1.43
2.320	.0511					
2.848		308	4.0	1.022	103	.690
2.985	.0477					

$M_\infty = 8.04$
$T_o = 669°K$
$Re_{D\infty} = 2.01 \times 10^5$
$p_o = 20.35$ ATM

$[(T_e-T_w)/T_e]_m = .446$
$\rho U/U_\infty = 1.19$
$U_\infty = 1116$ M/sec

x/D	$p/p_{\alpha=0}$	T_w °K	ΔT°K	$(T_e-T_w)/(T_{eff}-T_w)$	Nu_x	$Nu_x/\sqrt{Re_x}$
0	1.000	393	67.2	1.011	0	.793**
.098		400	70.5	1.015	48.4	.891
.164		389	62.3	1.004	70.6	.780
.257		379	56.0*	1.004	99.1	.741
.302	.637					
.393		369	50.7	.984	143	.880
.424	.410					
.518		349	34.5*	1.018	127	.763
.547	.225					
.658		333	21.9	1.010	104	.726
.720	.0790					
.785		324	17.3	1.011	100/123	.843/1.045
.805	.0489					
.869		322	15.5	1.016	122	1.095
.898	.0427					
1.652	.0309					
1.848		316*	9.5*	.993	162	1.155
2.320	.0298					
2.848		313	6.5	.998	171	1.024
2.985	.0262					

$M_\infty = 8.05$
$T_o = 669.4°K$
$Re_{D\infty} = 1.55 \cdot 10^5$
$p_o = 15.95$ ATM

$[(T_e-T_w)/T_e]_m = .453$
$\rho U/U_\infty = 1.185$
$U_\infty = 1122$ M/sec

x/D	$p/p_{\alpha=0}$	T_w °K	ΔT°K	$(T_e-T_w)/(T_{eff}-T_w)$	Nu_x	$Nu_x/\sqrt{Re_x}$
0	1.000	387	63.5	1.007	0	.809**
.098		393	65.7	1.010	43.8	.854
.164		380	56.5	.993	62.2	.735
.257		371	50.3*	1.002	87.2	.726
.302	.640					
.393		363	46.5	1.010	126	.848
.424	.400					
.518		344	31.5*	1.024	113	.739
.547	.213					
.658		328	19.0	1.002	89.1	.720
.720	.0729					
.785		321	15.0	1.005	86.1/106	.832/1.028
.805	.0518					
.869		323	17.7	1.004	140	1.39
.898	.0435					
1.652	.0318					
1.848		318*	13.0*	.997	219	1.75
2.320	.0303					
2.848		311	5.9	.999	152	.987
2.985	.0284					

* Temperature interpolation
** $Nu_D/(\rho U D^2/\mu)^{1/2}$

$M_\infty = 7.90$
$T_o = 670°K$
$Re_{D\infty} = 2.39 \times 10^5$
$p_o = 23.0$ ATM

$[(T_e-T_w)/T_e]_m = .440$
$\rho U/U_\infty = 1.19$
$U_\infty = 1117$ M/sec

x/D	$p/p_{\alpha=0}$	T_w °K	ΔT°K	$(T_e-T_w)/(T_{eff}-T_w)$	Nu_x	$Nu_x/\sqrt{Re_x}$
0	1.000	399	70.9	1.011	0	.777
.098		405	72.4	1.014	52.4	.856
.164		395	65.5	1.006	74.9	.761
.257		386	61.0*	1.004	109	.759
.302	.643					
.393		376	54.7	1.011	154	.858
.424	.415					
.518		354	37.2*	1.013	138	.764
.547	.227					
.658		336	24.0	1.006	115	.727
.720	.0800					
.785		327	18.4	1.009	107/132	.818/1.009
.805	.0490					
.869		324	16.0	1.004	123	1.040
.898	.0437					
1.652	.0309					
1.848		317*	10.0*	.990	170	1.154
2.320	.0239					
2.848		314	7.4	.987	196	1.198
2.985	.0214					

* Temperature interpolation
** $Nu_D/(\rho U D^2/\mu)^{1/2}$

$M_\infty = 7.93$ $[(T_e - T_w)/T_e]_m = .429$
$T_o = 672°K$ $\beta D/U_\infty = 1.19$
$Re_{D\infty} = 2.86 \times 10^5$ $U_\infty = 1120$ M/sec
$P_o = 28.0$ ATM

x/D	$p/p_{\alpha=0}$	T_w °K	ΔT °K	$(T_e-T_w)/(T_{eff}-T_w)$	Nu_x	$Nu_x/\sqrt{Re_x}$
0	1.000	413	78.0	1.008	0	.824**
.098		419	78.9	1.012	56.3	.890
.164		403	70.5	1.004	81.7	.767
.257		393	65.5*	1.004	119	.770
.302	.640					
.393		382	59.6	1.010	168	.873
.424	.413					
.518		358	40.4*	1.018	150	.761
.547	.224					
.658		339	26.2	1.021	**126**	**.738**
.720	.0782					
.785		329	20.4	1.007	118/146	.834/1.032
.805	.0482					
.869		327	18.3	1.003	135	1.018
.898	.0424					
1.652	.0291					
1.848		319*	12.0*	.988	205	1.290
2.320	.0224					
2.848		316	8.9	.983	**234**	1.368
2.985	.0195					

$M_\infty = 7.94$ $[(T_e - T_w)/T_e]_m = .652$
$T_o = 690°K$ $\beta D/U_\infty = 1.18$
$Re_{D\infty} = 1.30 \times 10^5$ $U_\infty = 1132$ M/sec
$P_o = 16.0$ ATM

x/D	$p/p_{\alpha=0}$	T_w °K	ΔT °K	$(T_e-T_w)/(T_{eff}-T_w)$	Nu_x	$Nu_x/\sqrt{Re_x}$
0	1.000	370	72.0	1.011	0	.758**
.098		375	71.8	1.006	42.7	.798
.164		358	64.6	1.016	64.1	.710
.257		344	56.5*	1.032	85.5	.640
.302	.636					
.393		325	48.1	1.037	107	.641
.424	.406					
.518		300	34.4*	1.045	107	.607
.547	.216					
.658		277	22.9	**1.060**	**92.2**	**.586**
.720	.0841					
.785		259	24.1	1.068	105/143	.798/.991
.805	.0668					
.869		254	19.2	1.060	127	.904
.898	.0506					
1.652	.0552					
1.848		238*	12.4*	1.015	176	1.01
2.320	.0312					
2.848		231	2.6	.991	57.6	.270
2.985	.0326					

$M_\infty = 7.90$ $[(T_e - T_w)/T_e]_m = .566$
$T_o = 696°K$ $\beta D/U_\infty = 1.175$
$Re_{D\infty} = .942 \times 10^5$ $U_\infty = 1138$ M/sec
$P_o = 9.23$ ATM

x/D	$p/p_{\alpha=0}$	T_w °K	ΔT °K	$(T_e-T_w)/(T_{eff}-T_w)$	Nu_x	$Nu_x/\sqrt{Re_x}$
0	1.000	340	57.9	1.008	0	.652**
.098		344	58.3	1.006	34.9	.785
.164		331	53.2	1.017	49.0	.656
.257		318	46.3*	1.034	66.7	.606
.302	.638					
.393		302	38.1	1.039	85.2	.608
.424	.516					
.518		281	27.3*	1.052	81.9	.563
.547	.227					
.658		263	17.4	1.069	65.3	.471
.720	.120					
.785		249	18.4	1.079	86.0/105	.714/.876
.805	.0970					
.869		244	14.1	1.070	90.6	.721
.898	.0652					
1.652						
1.848						
2.320	.0458					
2.848	.					
2.985	.0403					

* Temperature interpolation
** $Nu_D/(\beta D^2/\nu)^{1/2}$

$M_\infty = 8.06$ $[(T_e - T_w)/T_e]_m = .53$
$T_o = 702°K$ $\beta D/U_\infty = 1.17$
$Re_{D\infty} = 1.85 \times 10^5$ $U_\infty = 1144$ M/sec
$P_o = 20.0$ ATM

x/D	$p/p_{\alpha=0}$	T_w °K	ΔT °K	$(T_e-T_w)/(T_{eff}-T_w)$	Nu_x	$Nu_x/\sqrt{Re_x}$
0	1.000	373	70.1	1.010	0	.683**
.098		381	73.0	1.006	42.4	.748
.164		363	62.6	1.017	59.9	.631
.257		350	**59.8***	1.036	**91.1**	**.660**
.302	.638					
.393		329	**50.5**	1.041	**115**	**.634**
.424	.401					
.518		305	**38.5***	1.051	**117**	**.618**
.547	.217					
.658		282	**26.6**	**1.058**	**106**	**.640**
.720	.0802					
.785		261	23.8	1.062	113/139	.729/.896
.805	.0502					
.869		256	20.7	1.055	134	.869
.898	.0430					
1.652	.0393					
1.848		241*	8.5*	1.009	118	.429
2.320	.0267					
2.848		234	4.5	1.000	96.7	.222
2.985	.0286					

* Temperature interpolation
** $Nu_D/(\beta D^2/\nu)^{1/2}$

$M_\infty = 7.99$
$T_o = 698^oK$
$Re_{D\infty} = 2.15 \times 10^5$
$p_o = 23.3$ ATM

$[(T_e - T_w)/T_e]_m = .516$
$\beta D/U_\infty = 1.175$
$U_\infty = 1140$ M/sec

x/D	$p/p_{\alpha=0}$	T_w °K	ΔT °K	$(T_e-T_w)/(T_{eff}-T_w)$	Nu_x	$Nu_x/\sqrt{Re_x}$
0	1.000	388	78.2	1.011	0	.727**
.098		395	85.5	1.008	50.5	.838
.164		377	72.0	1.017	70.3	.667
.257		362	66.7*	1.038	103	.683
.302	.647					
.393		339	56.0	1.042	129	.669
.424	.412					
.518		313	**41.3***	1.053	**128**	**.634**
.547	.223					
.658		286	**27.3**	**1.059**	**108**	**.599**
.720	.0782					
.785		266	**27.3**	1.063	**127/157**	**.872/1.07**
.805	.0477					
.869		260	23.2	1.055	150	1.017
.898	.0415					
1.652	.0328					
1.848		243*	9.5*	1.018	132	.685
2.320	.0271					
2.848		236	5.3	.997	114	.462
2.985	.0269					

$M_\infty = 7.90$
$T_o = 684^oK$
$Re_{D\infty} = 2.74 \times 10^5$
$p_o = 27.5$ ATM

$[(T_e - T_w)/T_e]_m = .518$
$\beta D/U_\infty$ 1.188
$U_\infty = 1128$ M/sec

x/D	$p/p_{\alpha=0}$	T_w °K	ΔT °K	$(T_e-T_w)/(T_{eff}-T_w)$	Nu_x	$Nu_x/\sqrt{Re_x}$
0	1.000	395	81.5	1.012	0	.751**
.098		405	86.5	1.004	56.4	.867
.164		387	76.0	1.021	80.1	.723
.257		370	69.1*	1.020	114	.698
.302	.638					
.393		347	58.5	1.039	145	.690
.424	.412					
.518		318	**42.8***	1.053	**140**	[illegible]
.547	.221					
.658		291	**29.8**	1.063	**124**	**.625**
.720	.0766					
.785		269	28.6	1.056	142/175	.878/1.081
.805	.0467					
.869		263	24.0	1.050	163	1.025
.898	.0407					
1.652	.0302					
1.848		245*	10.0*	1.008	145	.732
2.320	.0214					
2.848		239	5.5	.990	124	.523
2.985	.0243					

* Temperature interpolation
** $Nu_D/(\beta D^2/\nu)^{1/2}$

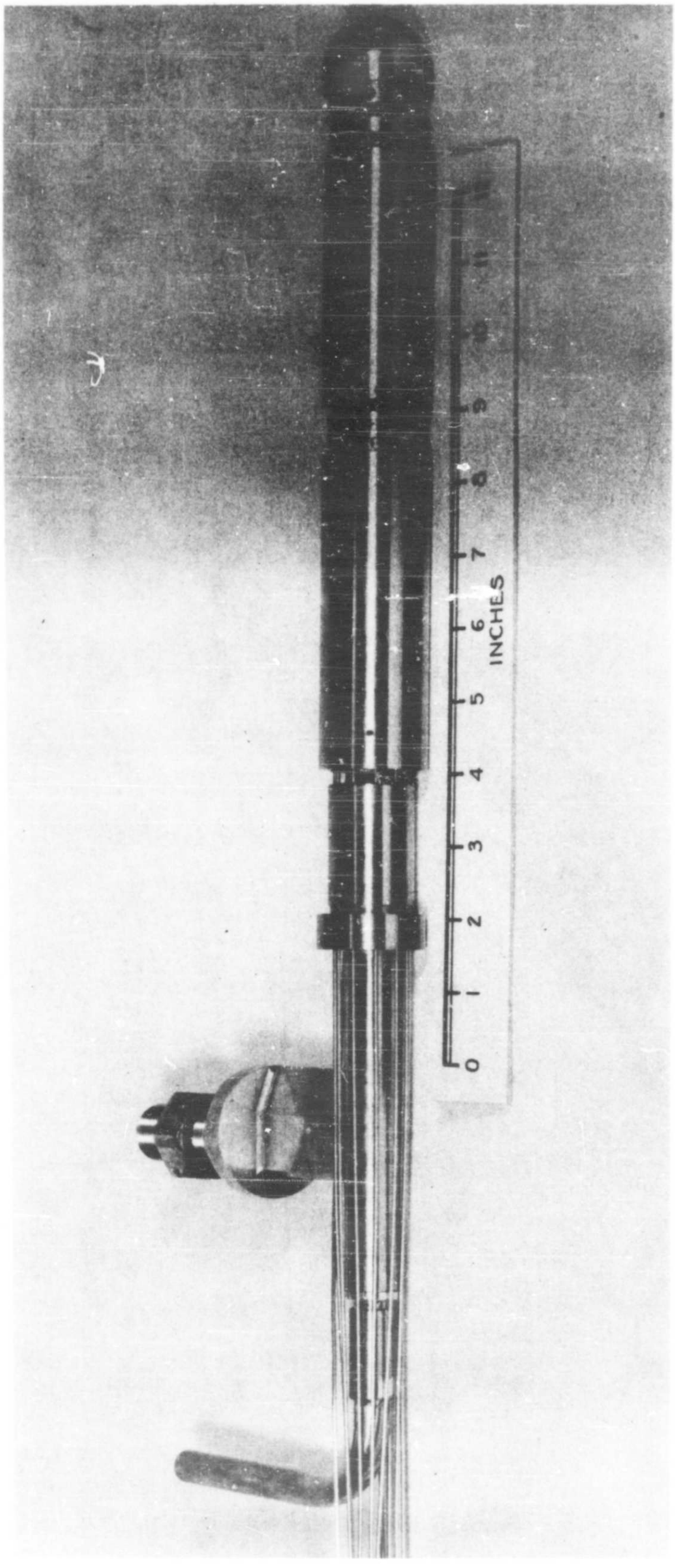

FIG. I HEMISPHERE - CYLINDER PRESSURE MODEL

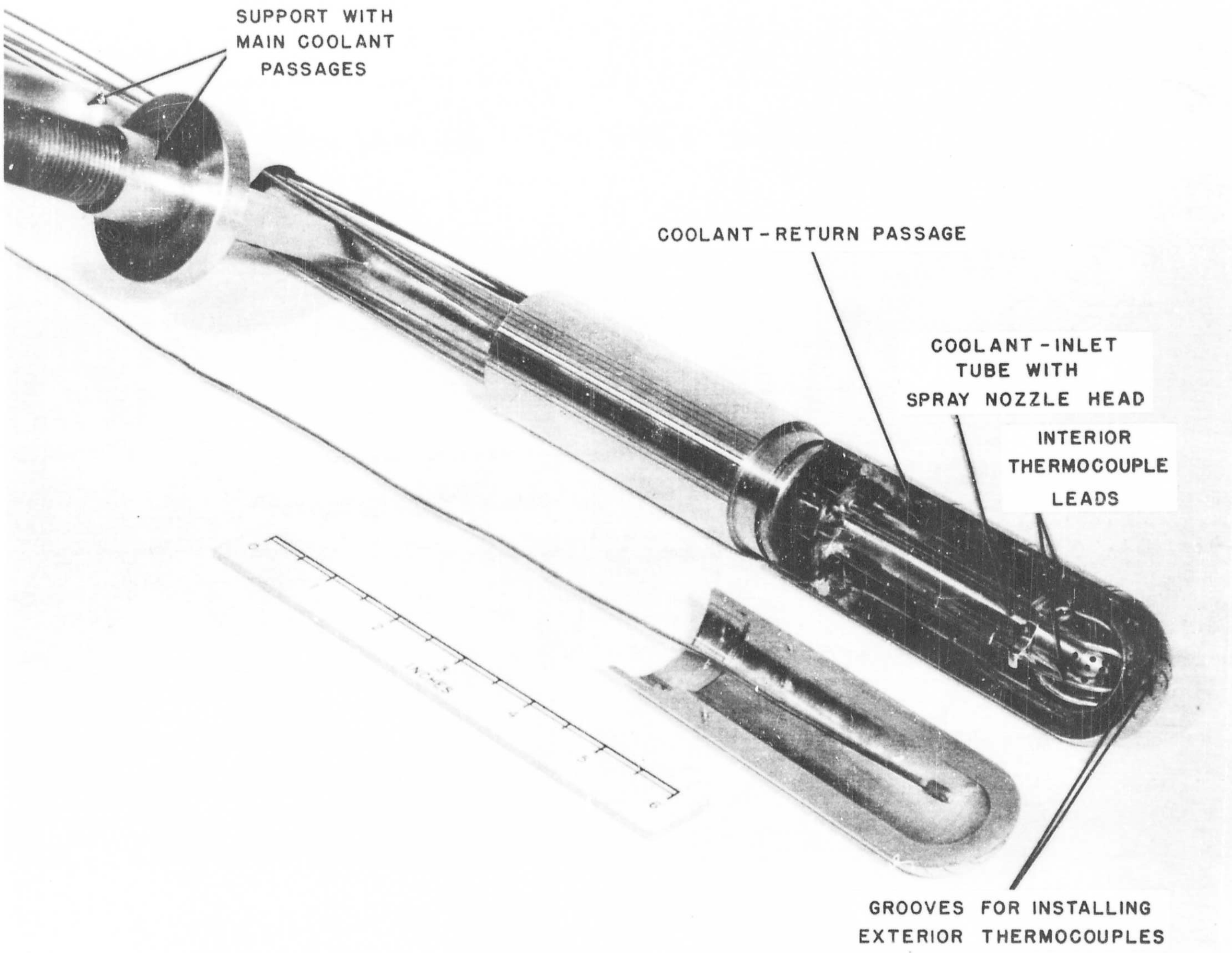

FIG. 2 CUT - AWAY VIEW OF HEMISPHERE - CYLINDER HEAT TRANSFER MODEL

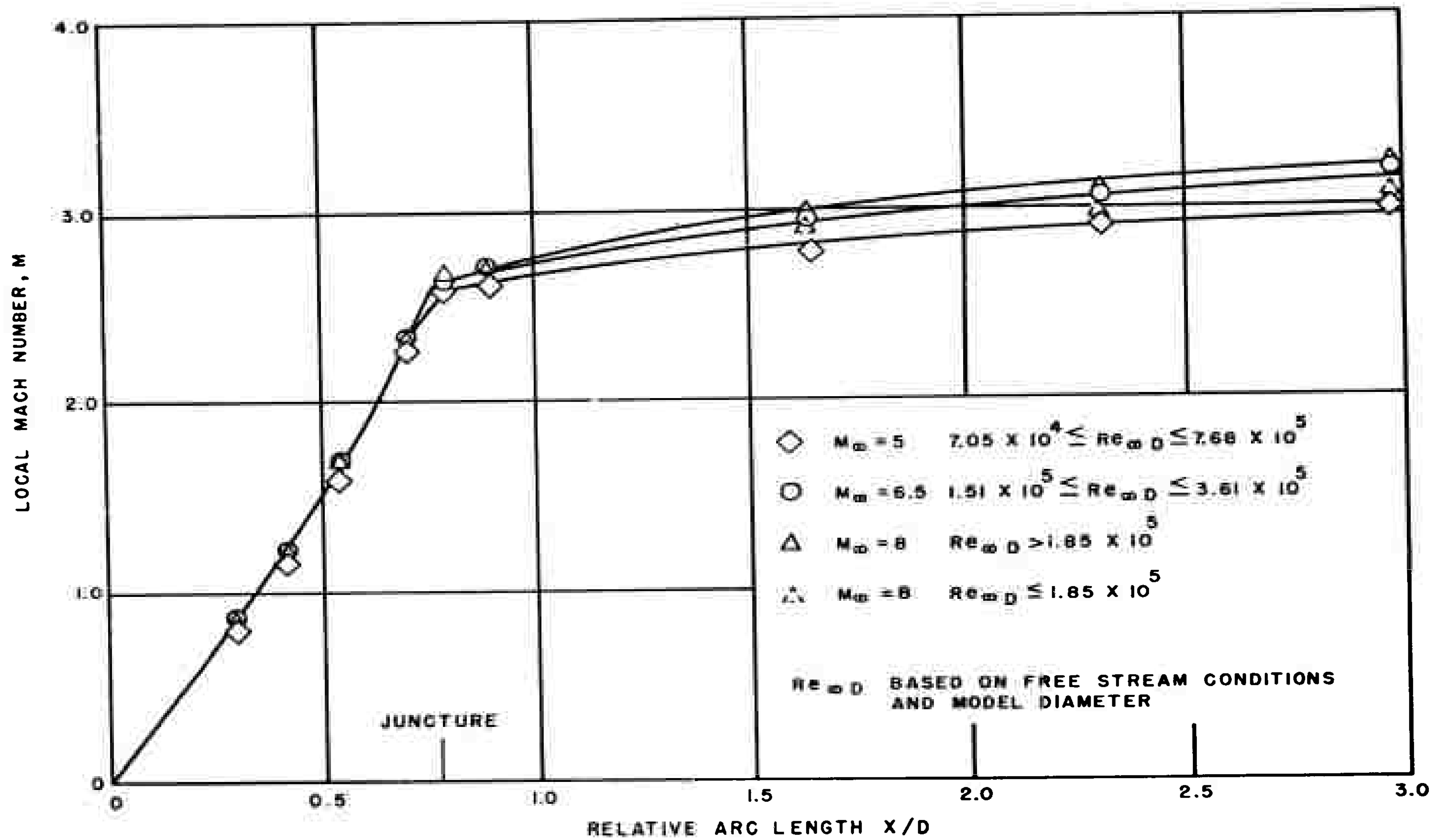

FIG. 3 MACH NUMBER DISTRIBUTION OVER HEMISPHERE CYLINDER

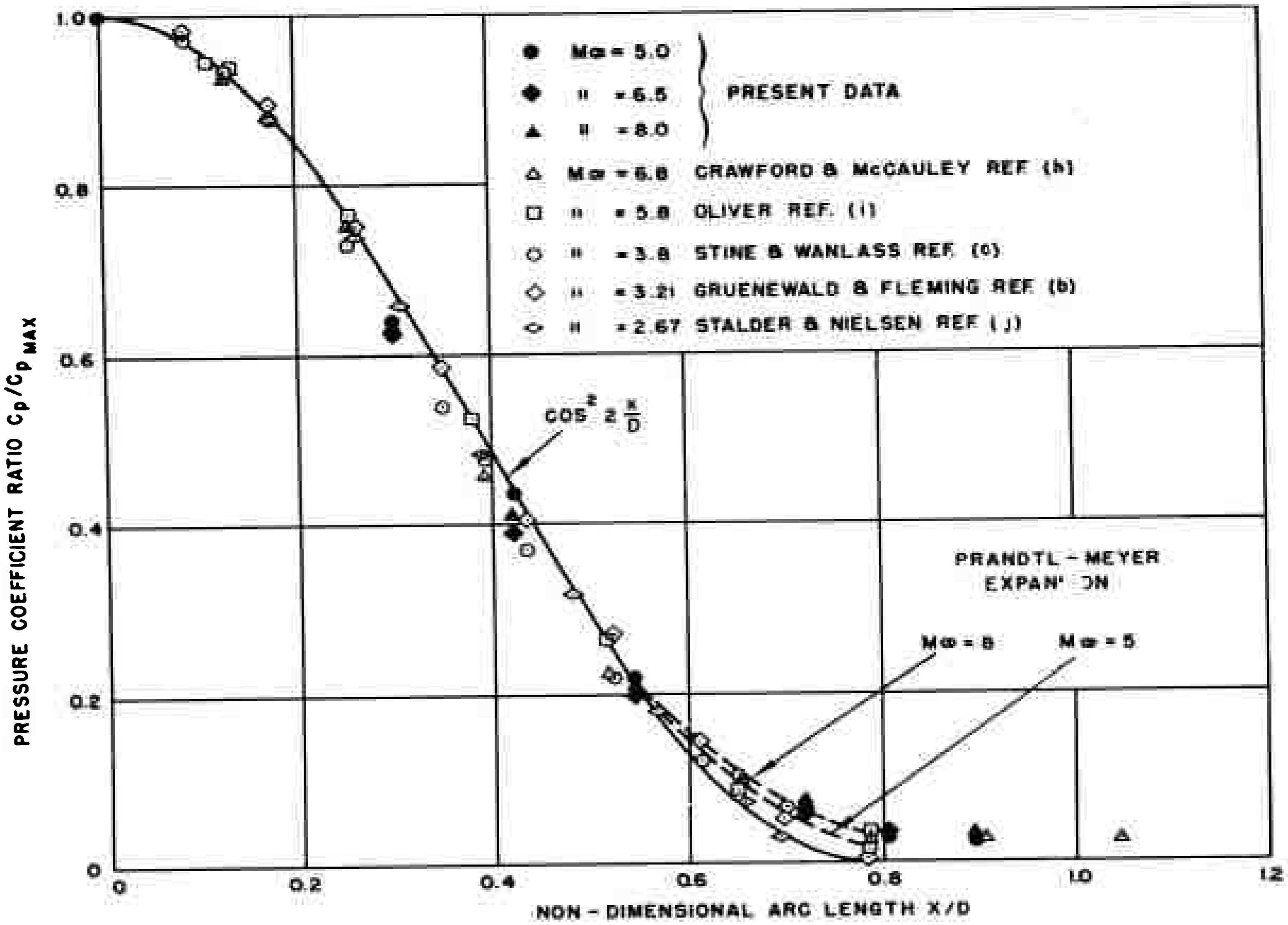

FIG. 4 PRESSURE COEFFICIENT DISTRIBUTION OVER HEMISPHERE-CYLINDER AT VARIOUS MACH NUMBERS

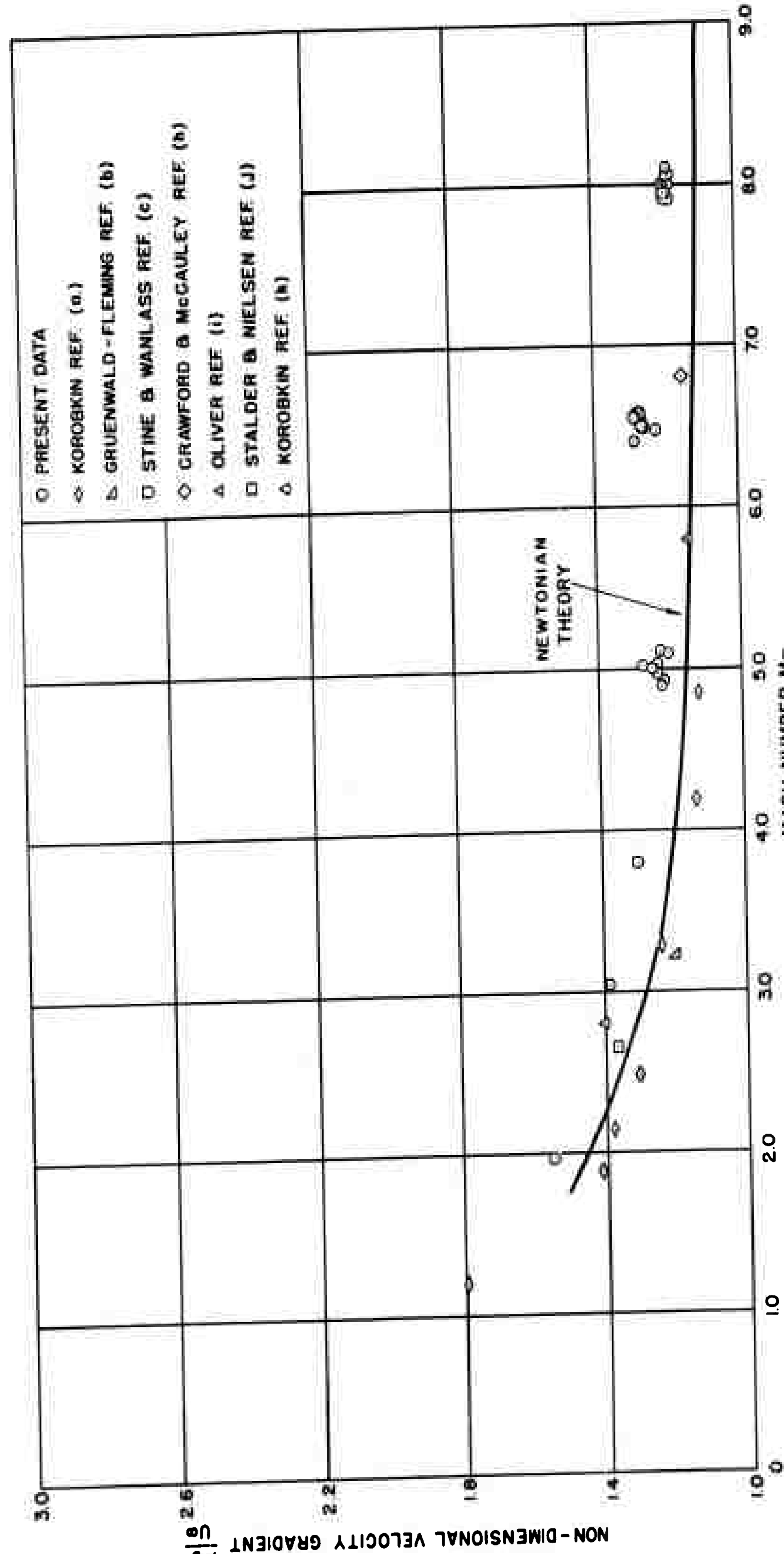

FIG. 5 NON-DIMENSIONAL VELOCITY GRADIENT AT MODEL STAGNATION POINT VS FREE-STREAM MACH NUMBER

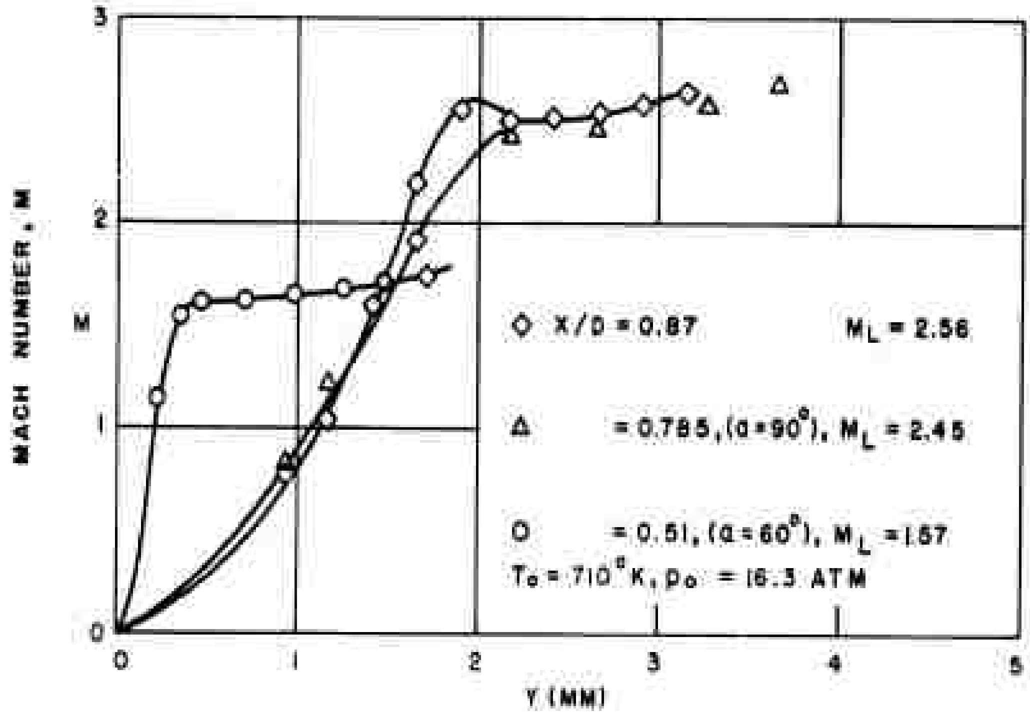

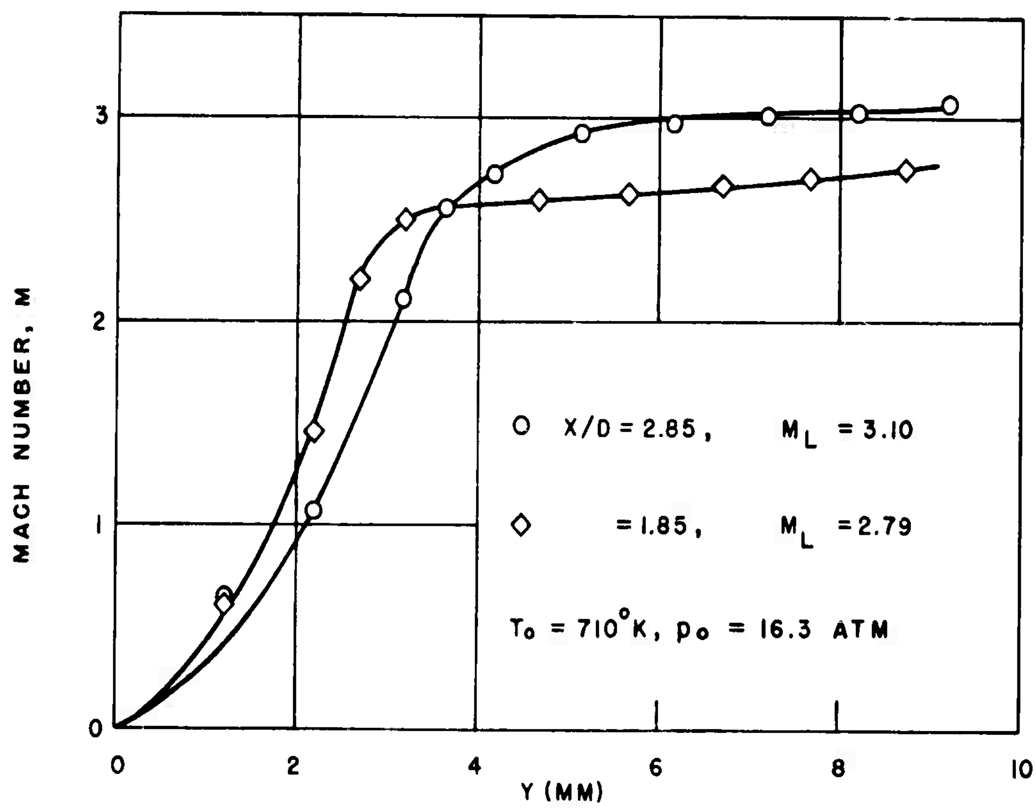

FIG. 6 MACH NUMBER DISTRIBUTION ACROSS BOUNDRY LAYER AT VARIOUS STATIONS ON THE HEMISPHERE-CYLINDER FOR A FREE-STREAM MACH NUMBER OF 8

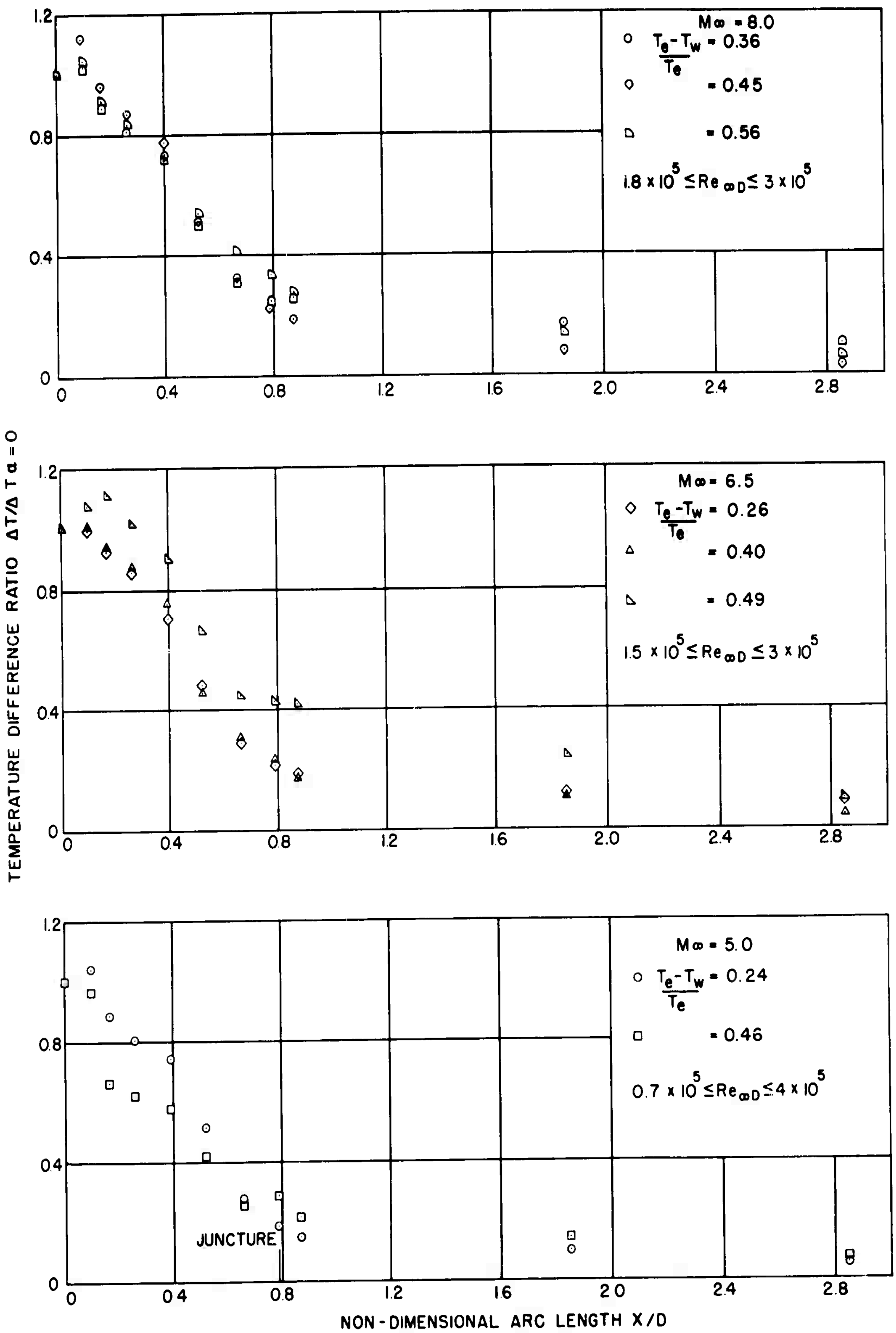

FIG. 7 VARIATION OF TEMPERATURE DIFFERENCE RATIO OVER HEMISPHERE-CYLINDER

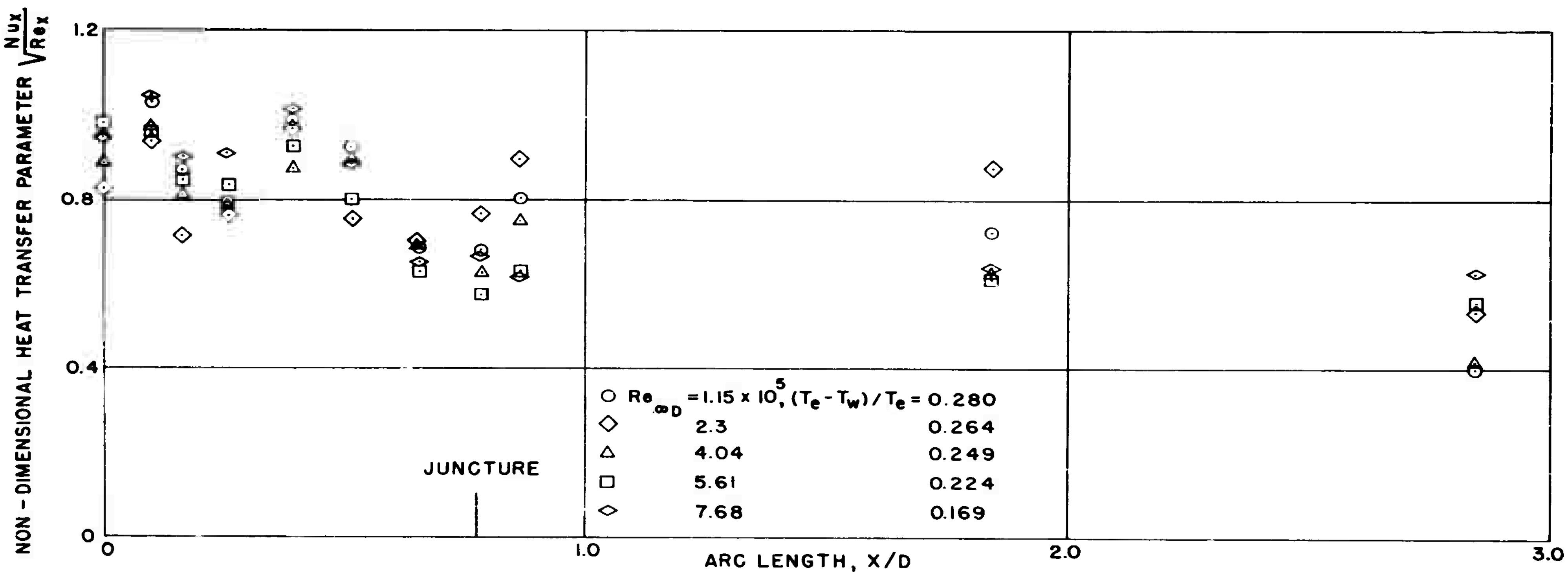

FIG. 8a NON-DIMENSIONAL HEAT-TRANSFER-PARAMETER DISTRIBUTION OVER HEMISPHERE - CYLINDER

MACH NUMBER AND $T_w / T_e \sim 0.725$

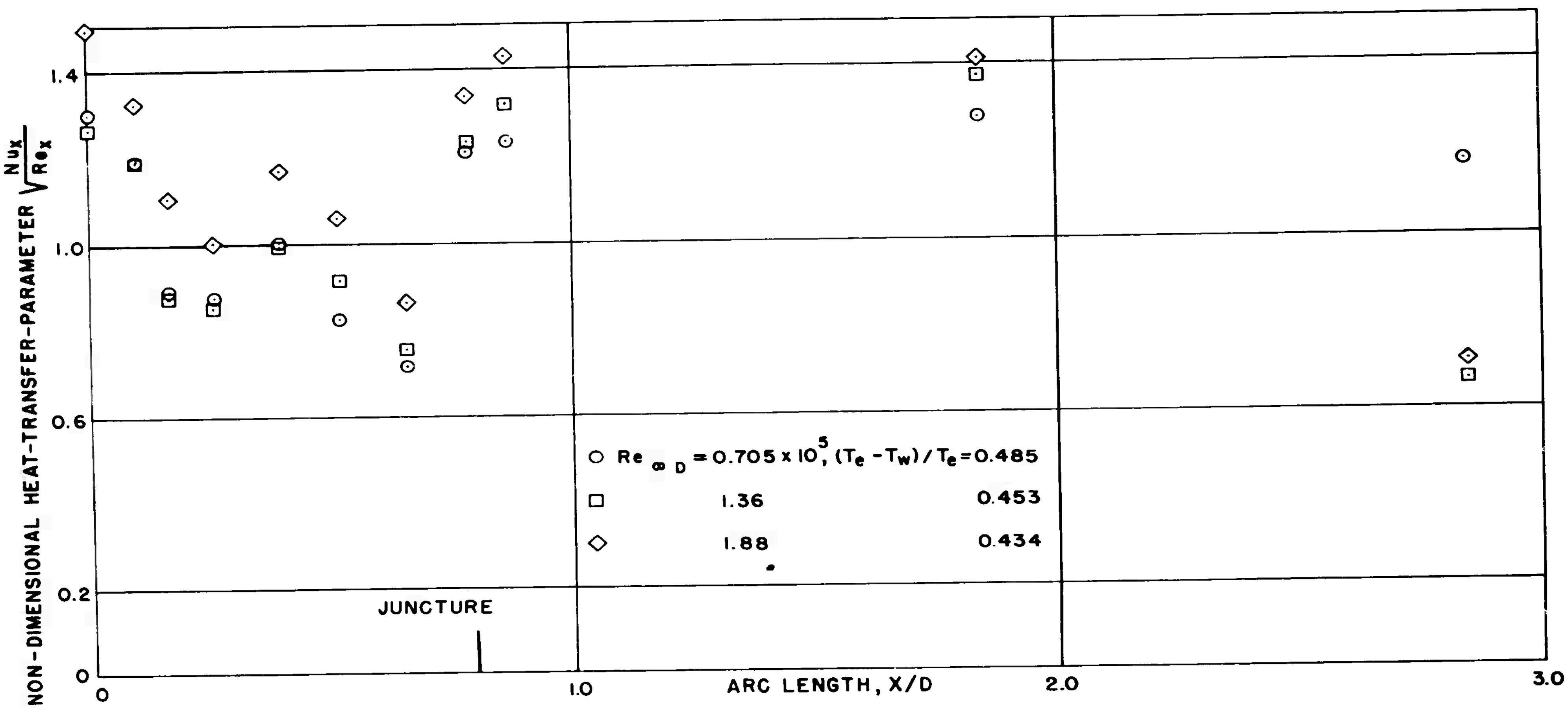

FIG. 8b NON-DIMENSIONAL HEAT-TRANSFER-PARAMETER DISTRIBUTION OVER HEMISPHERE-CYLINDER

MACH NUMBER 5 AND $T_w / T_e \sim 0.517$

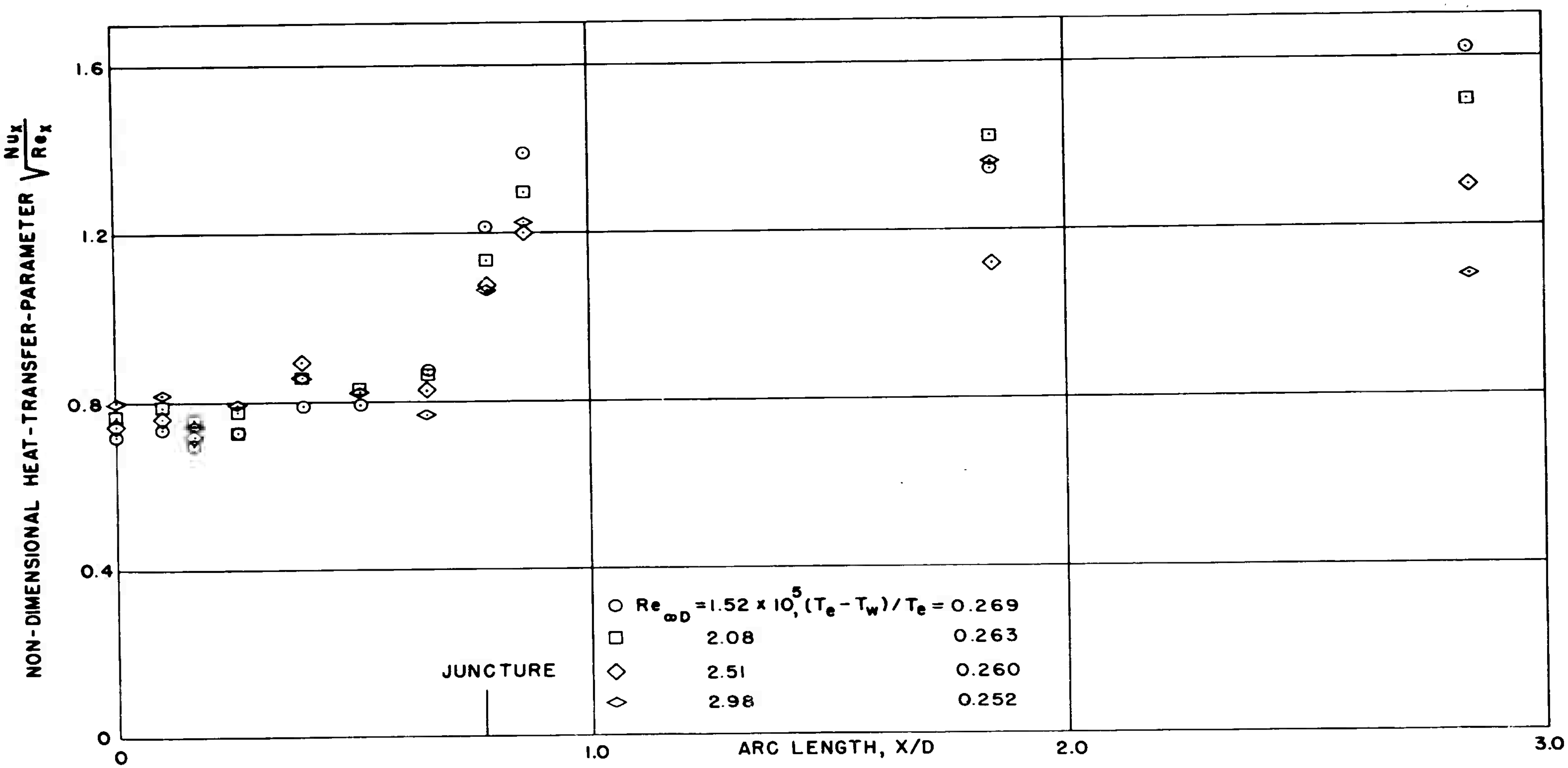

FIG. 8c NON-DIMENSIONAL HEAT-TRANSFER-PARAMETER DISTRIBUTION OVER HEMISPHERE-CYLINDER

MACH NUMBER 6.5 AND $T_w/T_e \sim 0.697$

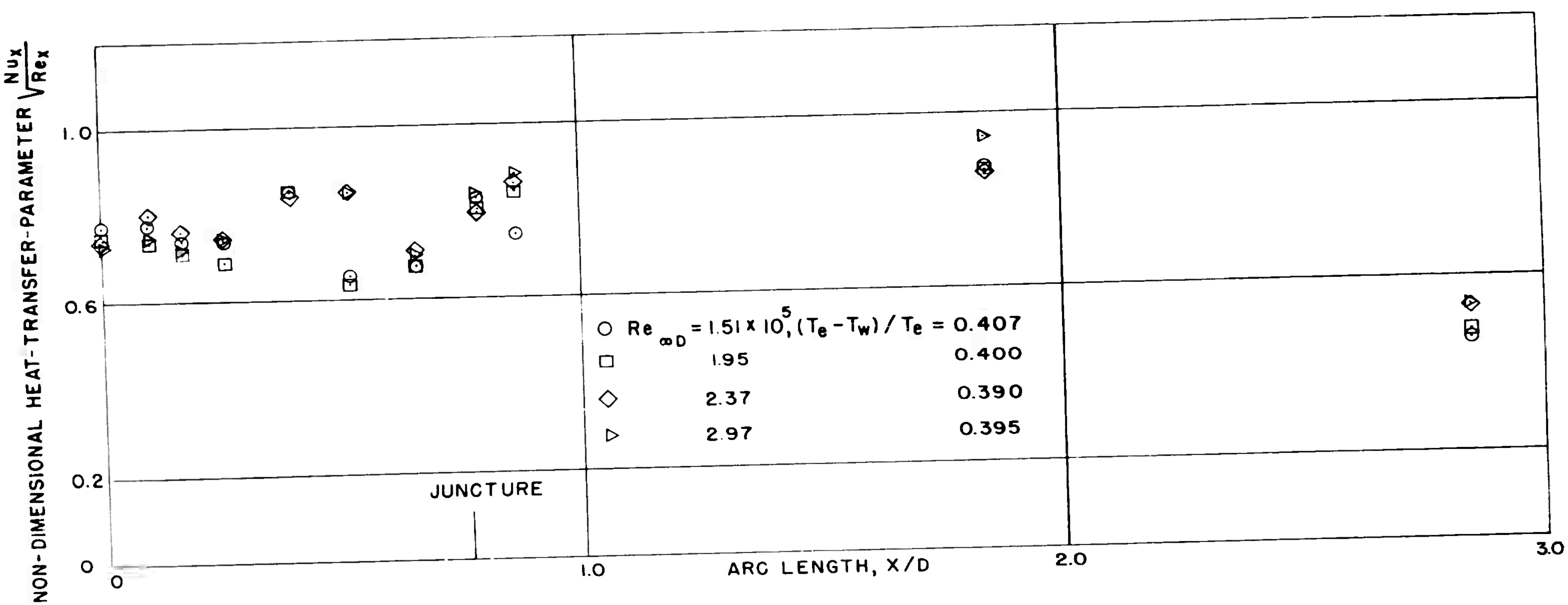

FIG. 8d NON-DIMENSIONAL HEAT-TRANSFER-PARAMETER DISTRIBUTION OVER HEMISPHERE - CYLINDER

MACH NUMBER 6.5 AND $T_w/T_e \sim 0.565$

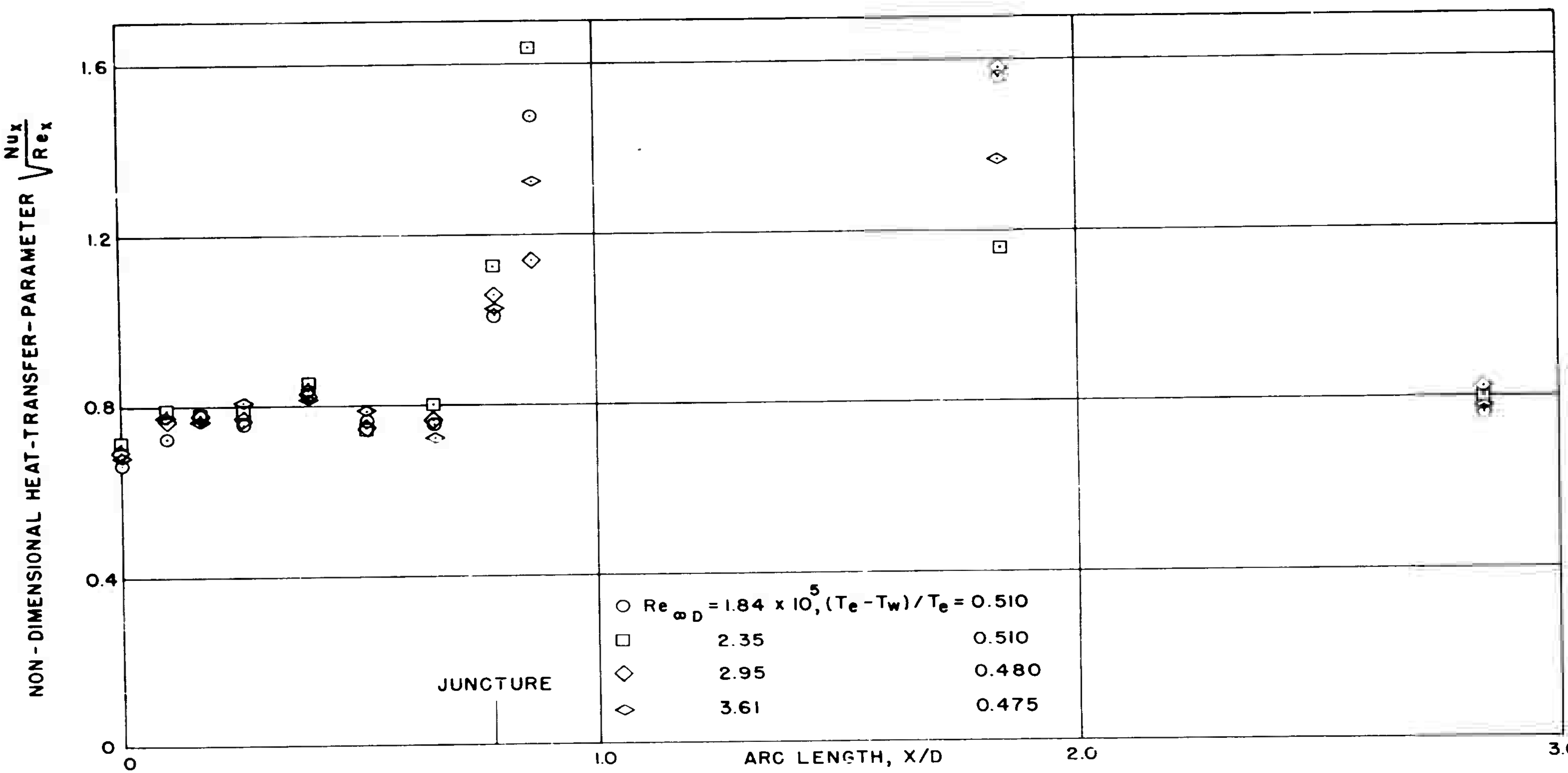

FIG. 8e NON-DIMENSIONAL HEAT-TRANSFER-PARAMETER DISTRIBUTION OVER HEMISPHERE-CYLINDER

MACH NUMBER 6.5 AND $T_w/T_e \sim 0.474$

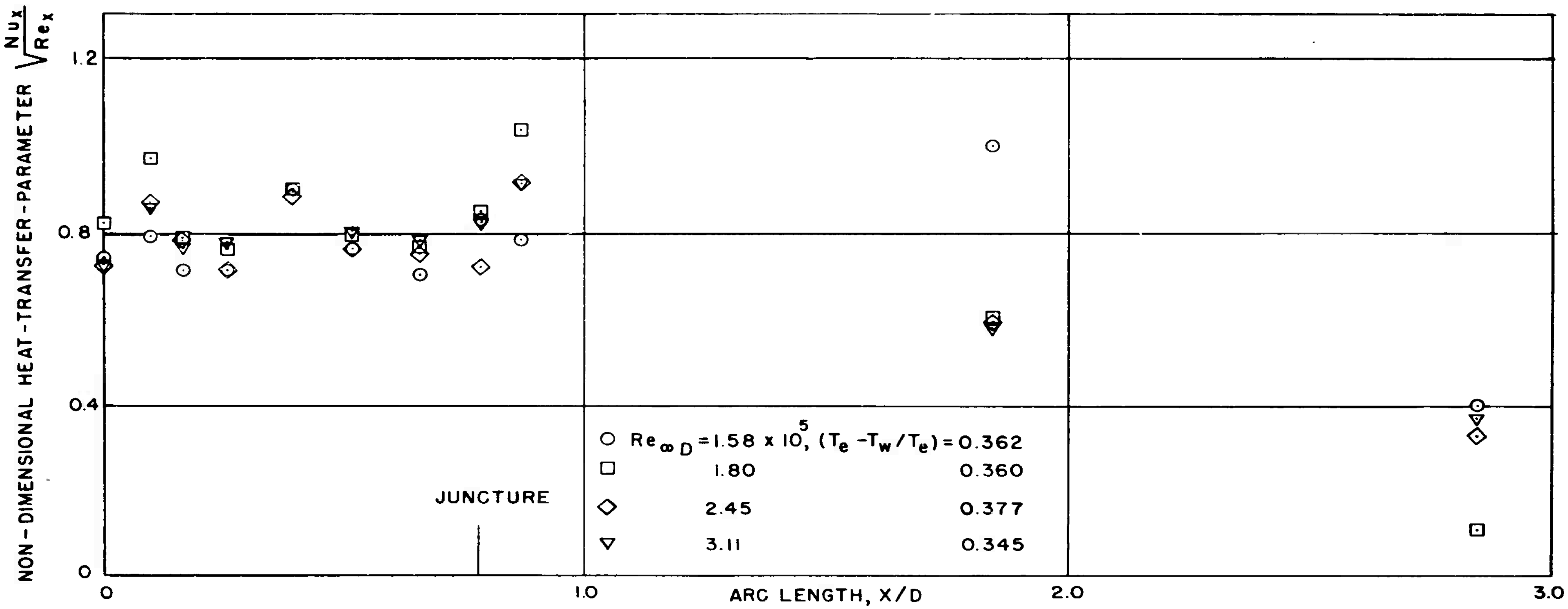

FIG. 8f NON-DIMENSIONAL HEAT-TRANSFER-PARAMETER DISTRIBUTION OVER HEMISPHERE-CYLINDER

MACH NUMBER 8 AND $T_w/T_e \sim 0.613$

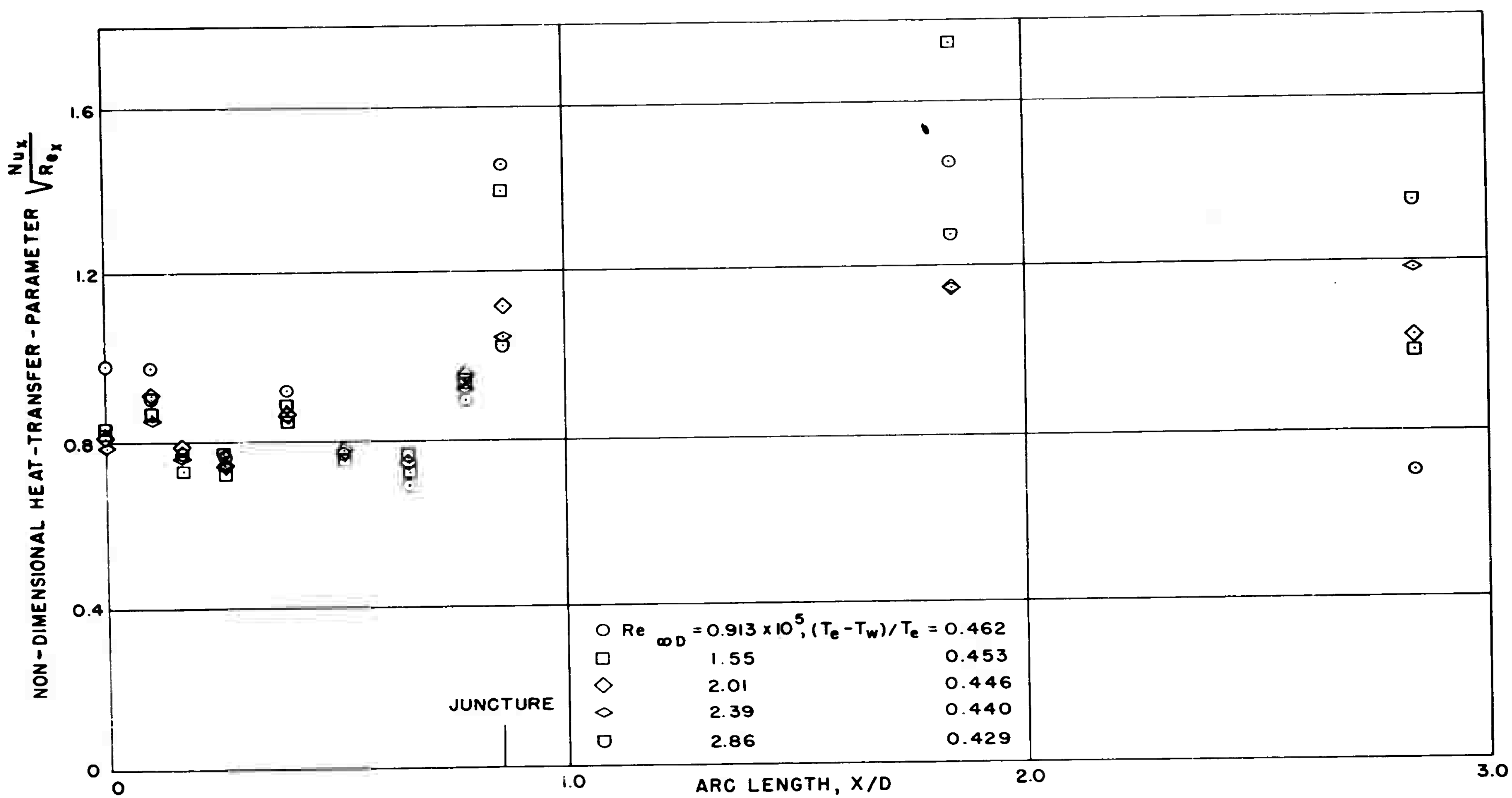

FIG. 8g NON-DIMENSIONAL HEAT-TRANSFER-PARAMETER DISTRIBUTION OVER HEMISPHERE-CYLINDER

MACH NUMBER 8 AND $T_w/T_e \sim 0.522$

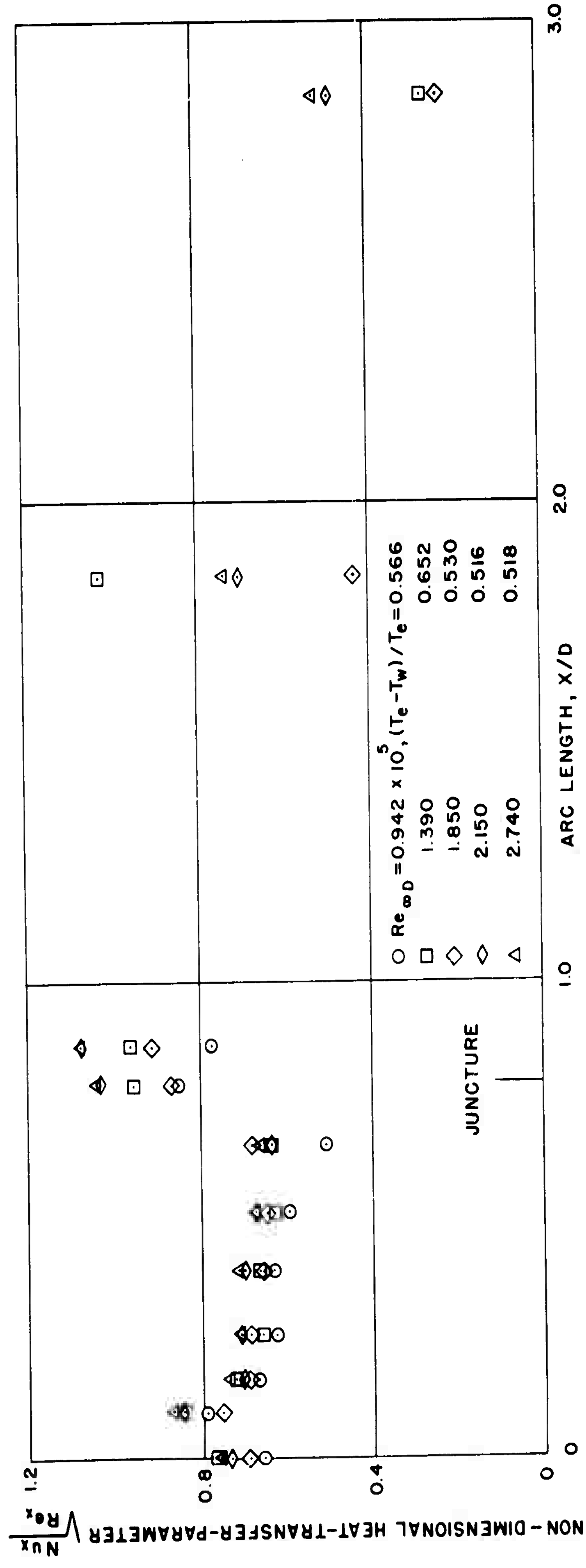

FIG. 8h NON-DIMENSIONAL HEAT-TRANSFER-PARAMETER DISTRIBUTION OVER HEMISPHERE-CYLINDER

MACH NUMBER 8 AND $T_w/T_e \sim 0.440$

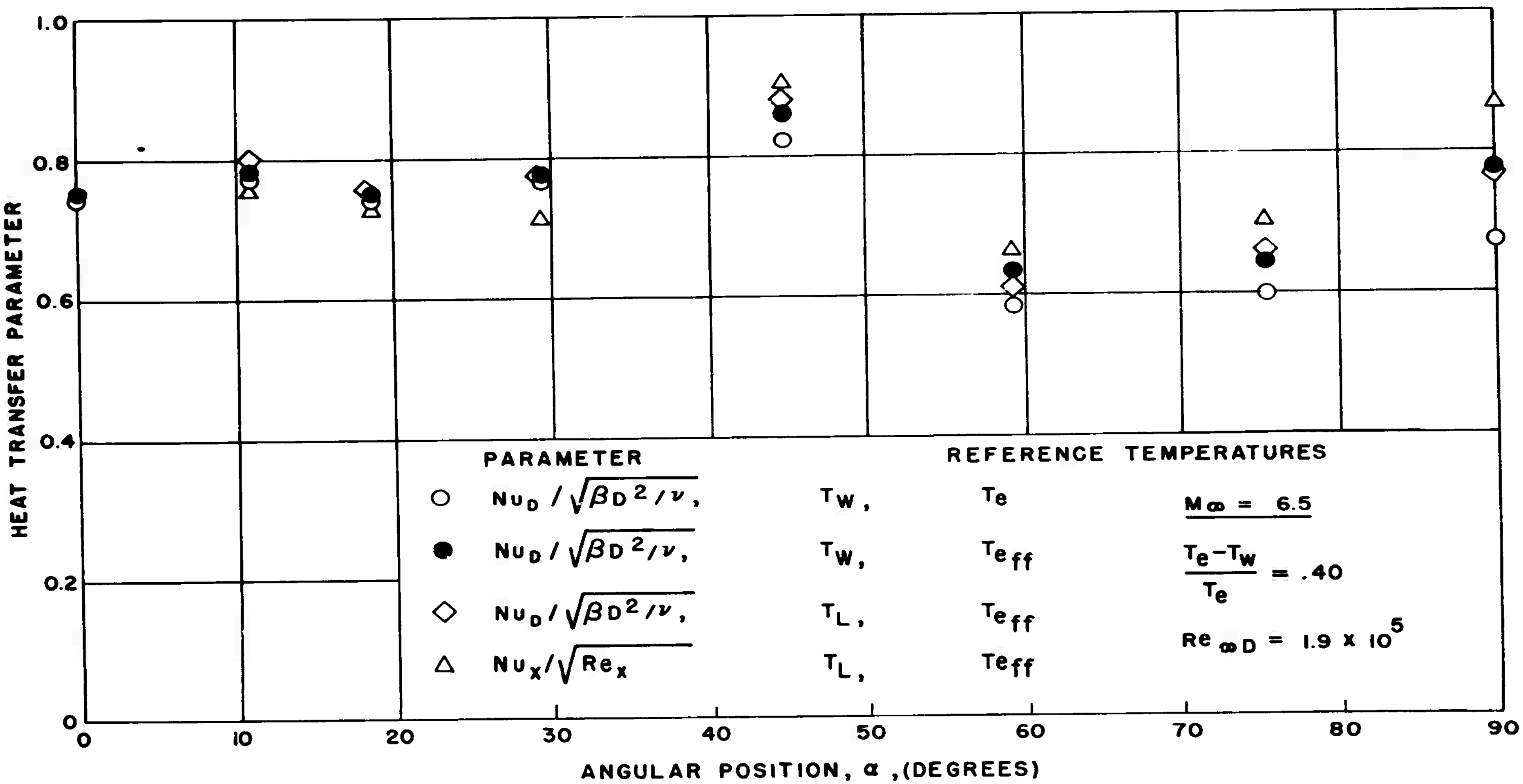

FIG. 9 COMPARISON OF HEAT-TRANSFER PARAMETERS COMPUTED ON THE BASIS OF DIFFERENT REFERENCE VALUES

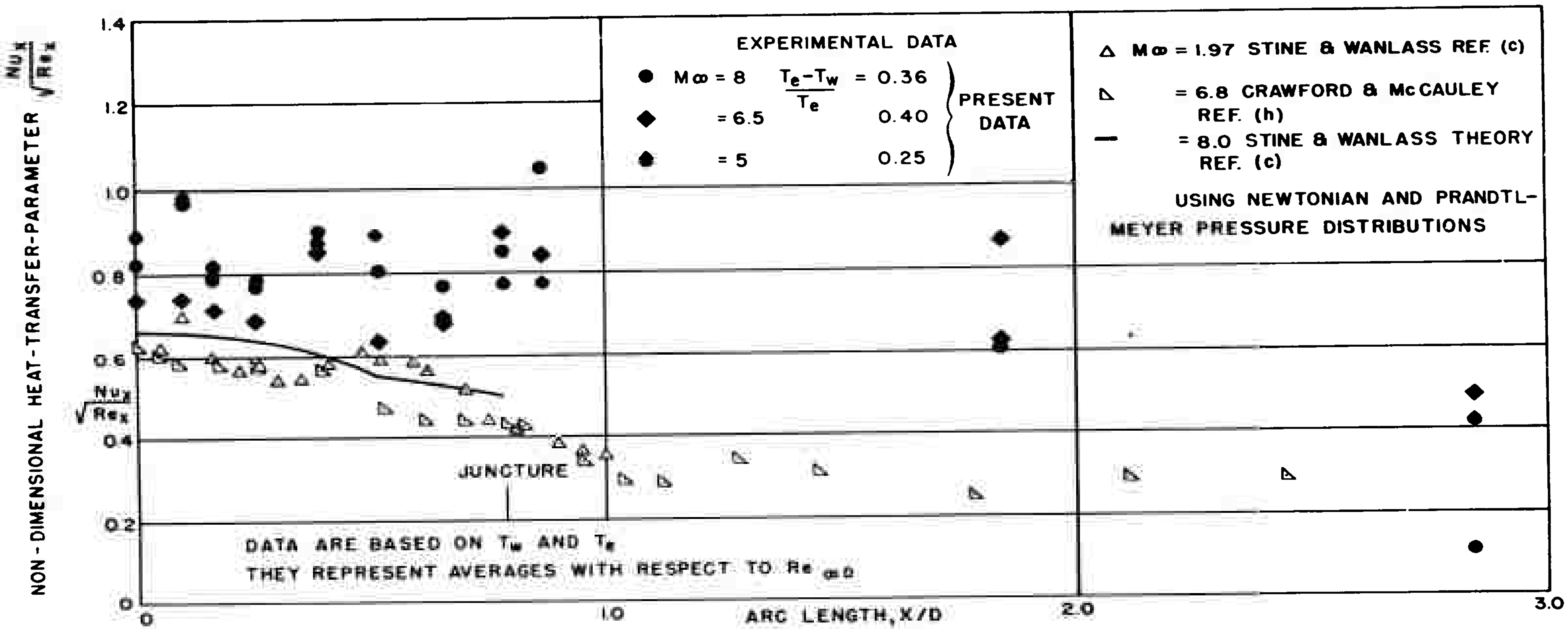

FIG. 10a COMPARISON OF PRESENT DATA WITH OTHER EXPERIMENTAL DATA AND WITH THEORY

$\frac{Nu_x}{\sqrt{Re_x}}$ VS ARC LENGTH x/D

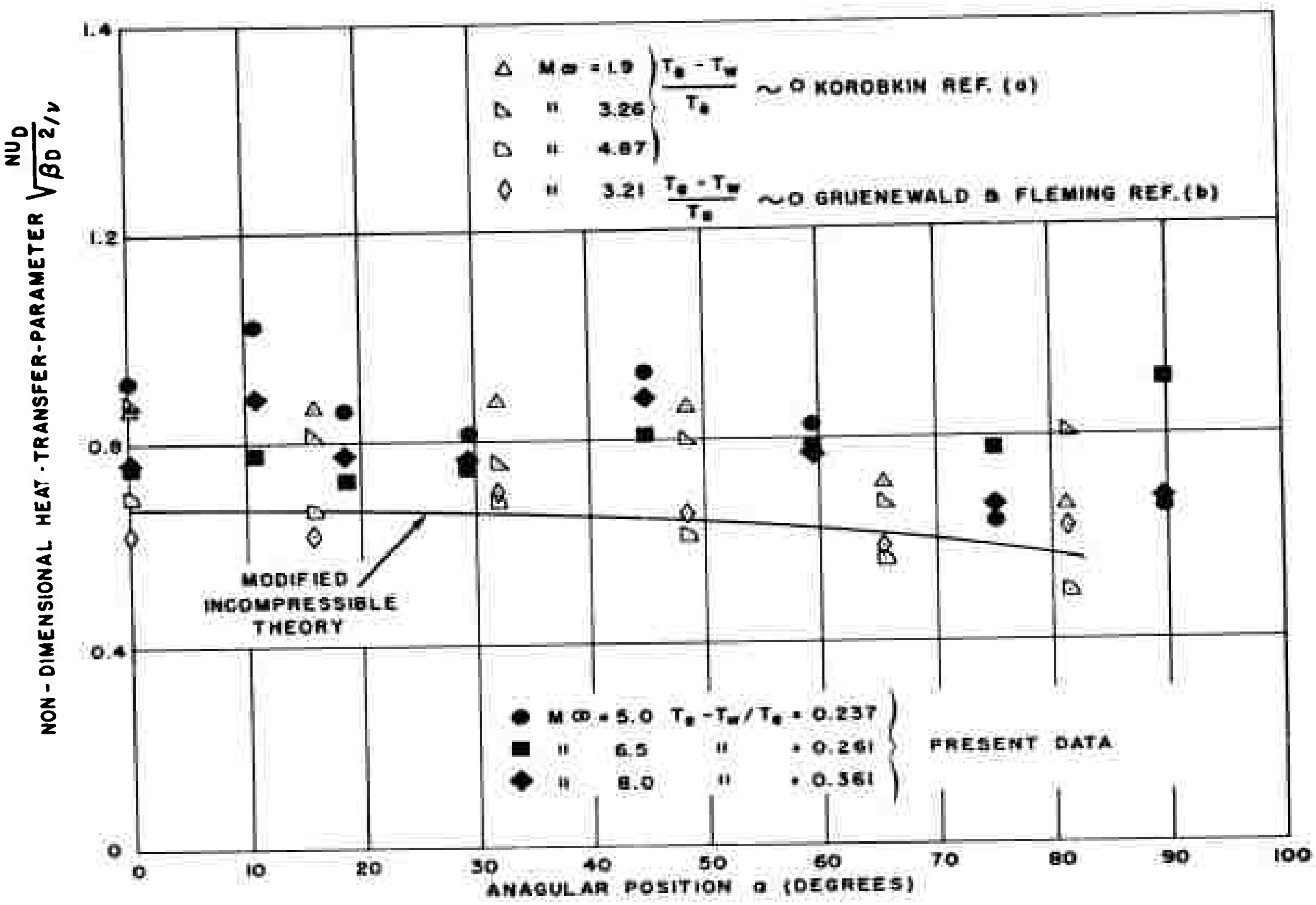

FIG. 10b COMPARISON OF PRESENT DATA WITH OTHER EXPERIMENTAL DATA AND WITH THEORY

$\frac{Nu_D}{\sqrt{BD^2/\nu}}$ VS ANGULAR POSITION α

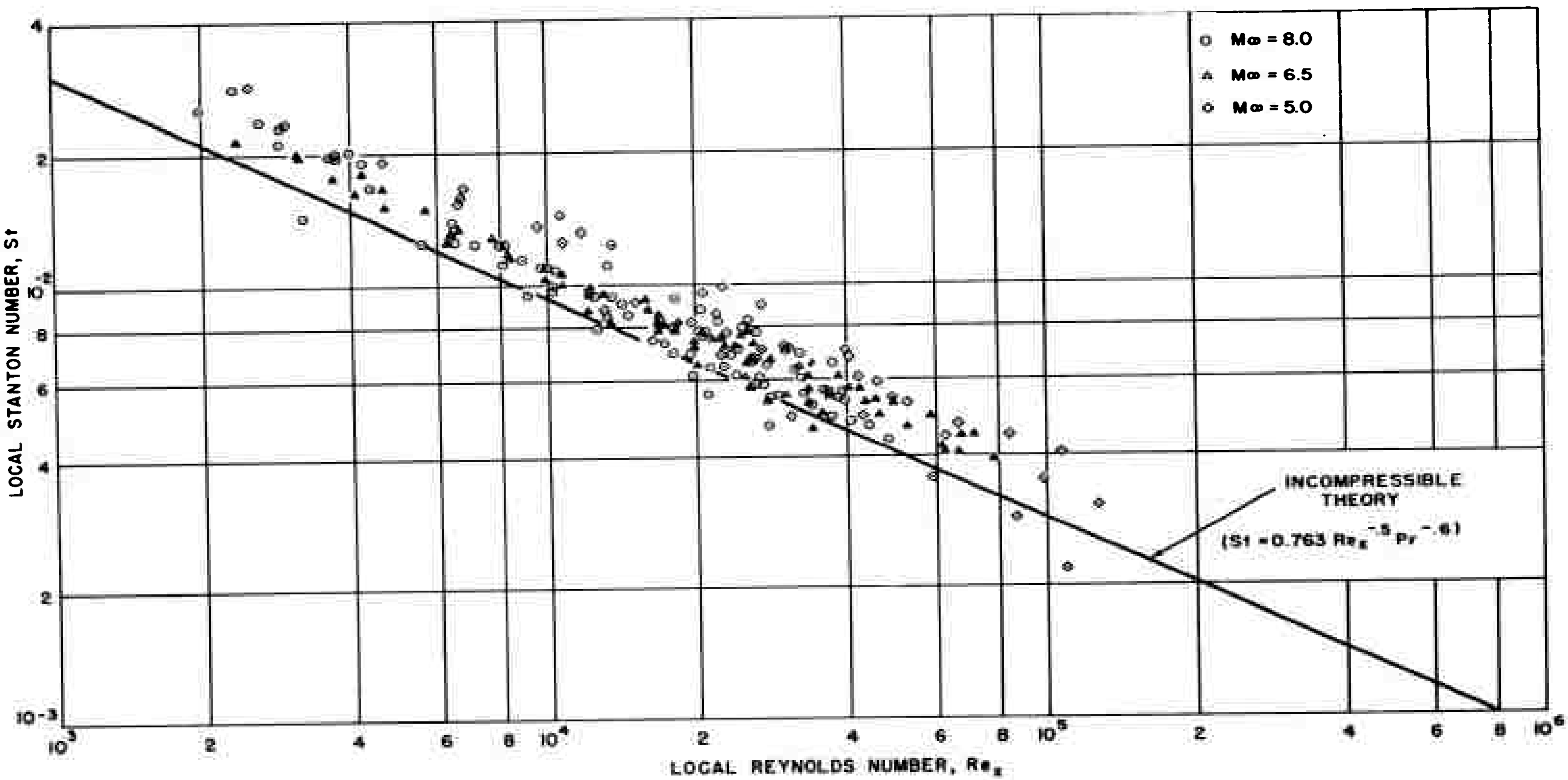

FIG. 11 VARIATION OF LOCAL STANTON NUMBER WITH LOCAL REYNOLDS NUMBER ALONG HEMISPHERE (Pr =0.70)

Aeroballistic Research Department
External Distribution List for Aeroballistic Research

No. of Copies	
	Chief, Bureau of Ordnance Department of the Navy Washington 25, D. C.
1	Attn: Ad3
1	Attn: Ree
1	Attn: Re03
1	Attn: ReS1e
	Chief, BuAer Washington 25, D. C.
3	Attn: TD-414
	Commander, U. S. NOTS Inyokern, China Lake, California
1	Attn: Technical Library
1	Attn: Code 503
	Commander, NAMTC Point Mugu, California
2	Attn: Technical Library
	Superintendent U. S. Naval Postgraduate School Monterey, California
1	Attn: Tech. Rpts Section, Library
	Director, NRL Washington 25, D. C.
1	Attn: Code 2021
	Officer in Charge, NPG Dahlgren, Virginia
1	Attn: Technical Library
	Office, Chief of Ordnance Department of the Army Washington 25, D. C.
1	Attn: ORDTU
	Office of the Assistant Secretary of Defense (R and D) Room 3 E 1065, The Pentagon Washington 25, D. C.
1	Attn: Technical Library

No. of Copies	
	Chief, AFSWP Washington 25, D. C.
1	Attn: Document Library Br.
	Commander, WADC Wright-Patterson AF Base Ohio
5	Attn: WCOSI-3
3	Attn: WCRRD
1	Attn: WCLGH-3
1	Director Air University Library Maxwell AF Base, Alabama
	Commanding General Aberdeen Proving Ground, Maryland
1	Attn: Technical Info. Br.
1	Attn: Ballistics Res. Lab.
	Commanding General Redstone Arsenal Huntsville, Alabama
1	Attn: Aero. Lab, GMDD
10	ASTIA Document Service Center Knott Building Dayton 2, Ohio
	NACA High Speed Flight Station Box 273 Edwards Air Force Base, California
1	Attn: Mr. W. C. Williams
	NACA Ames Aeronautical Laboratory Moffett Field, California
1	Attn: Librarian
	NACA Langley Aeronautical Lab. Langley Field, Virginia
2	Attn: Librarian
1	Attn: Adolf Busemann
1	Attn: John J. Stack

No. of Copies	
1	CONVAIR Corporation A Div. of Gen. Dynamics Corp. Daingerfield, Texas
1	United Aircraft Corporation 400 Main Street East Hartford 8, Connecticut Attn: Chief Librarian
1	Cornell Aeronautical Lab., Inc. P. O. Box 235, 4455 Genessee St. Buffalo 21, New York Attn: Librarian
1	Lewis Flight Propulsion Lab. 21000 Brookpark Road Cleveland 11, Ohio Attn: Chief, Supersonic Propulsion Division
2	Armour Research Foundation 10 West 35th Street Chicago 16, Illinois Attn: Dept. M.
1	Hughes Aircraft Company Florence Ave. at Teale St. Culver City, California Attn: Mr. Dana H. Johnson R & D Technical Library
1	McDonnell Aircraft Corporation P. O. Box 516 St. Louis 3, Missouri
2	General Electric Company Missile & Ordnance Systems Dept. 3198 Chestnut Street Philadelphia 4, Pennsylvania Attn: Larry Chasen Manager, Library
2	Eastman Kodak Company Navy Ordnance Division 50 West Main Street Rochester 14, New York Attn: Mr. W. B. Forman

No. of Copies	
1	Lockheed Aircraft Corporation Missile Systems Division Palo Alto, California Attn: Mr. D. L. H. Wilson
1	Chief, Fluid Mechanics Section National Bureau of Standards Washington 25, D. C.
1	National Bureau of Standards Washington 25, D. C. Attn: Applied Math. Div.
1	Commanding Officer Office of Naval Research Br. Off. Box 39, Navy 100 Fleet Post Office New York, New York
1	Langley Aeronautical Laboratory Langley Field, Virginia Attn: Theoretical Aerodynamics Division
1	Case Institute of Technology Cleveland 6, Ohio Attn: G. Kuerti
1	Massachusetts Institute of Tech. Cambridge 39, Mass. Attn: Prof. Joseph Kaye Room 1-212
1	The Johns Hopkins University Charles and 34th Streets Baltimore 18, Maryland Attn: Dr. Francis H. Clauser
2	Director Inst. for Fluid Dynamics and Applied Mathematics University of Maryland College Park, Maryland
1	Cornell University Graduate School of Aero. Eng. Ithaca, New York Attn: Prof. W. R. Sears

No. of Copies		No. of Copies	
1	NACA Lewis Flight Propulsion Lab. 21000 Brookpark Road Cleveland 11, Ohio Attn: Librarian	1	University of Michigan Willow Run Research Center Willow Run Airport Ypsilanti, Michigan Attn: Librarian
1	NACA 1512 H Street N. W. Washington 25, D. C. Attn: Bertram A. Muleahy Chief, Div. of Research Information	1	University of Michigan Ann Arbor, Michigan
1	Commanding Officer, DOFL Washington 25, D. C. Attn: Lib., Rm 211, Bldg. 92	2	APL/JHU 8621 Georgia Avenue Silver Spring, Maryland Attn: Tech. Rpts. Group
1	Office of Naval Research Room 2709, T-3 Building Washington 25, D. C. Attn: Head, Mechanics Br.	1	The Ohio State University Research Foundation Nineteenth Avenue Columbus 10, Ohio Attn: Security Officer
1	Director of Intelligence Headquarters, USAF Washington 25, D.C. Attn: AFOIN-3B	 1 2 1	CIT Pasadena 4, California Attn: Aeronautics Dept. Attn: Jet Propulsion Lab Attn: Guggenheim Aeronautical Laboratory, Aeronautics Library
1	Director, DTMB Aerodynamics Laboratory Washington 7, D. C. Attn: Library	1	University of Minnesota Minneapolis 14, Minnesota Attn: Mechanical Eng. Dept.
  1 2	University of California Berkeley 4, California Attn: G. J. Maslach, 205-T3 Attn: Dr. S. A. Schaaf	1	BAR Aeroject-General Corporation 6352 N. Irwindale Avenue Azusa, California
1	Defense Research Laboratory The University of Texas P. O. Box 8029 Austin 12, Texas Attn: H. D. Krick, Asst.Dir.	1	RAND Corp. 1700 Main Street Santa Monica, California Attn: Lib., USAF Project RAND
1	Applied Math. and Statistics Lab. Stanford University Stanford, California	1	Douglas Aircraft Company Inc. Santa Monica Division 3000 Ocean Park Boulevard Santa Monica, California Attn: Chief Engineer

No. of Copies	
	AER, Incorporated 871 East Washington Street Pasadena, California
1	Attn: Dr. A. J. A. Morgan
	Princeton University James Forrestal Research Center Gas Dynamics Laboratory Princeton, New Jersey
1	Attn: Prof. S. M. Bogdonoff
	Commanding General Army Ballistic Missile Agency Huntsville, Alabama
1	Attn: ORDAB-DA
1	The AVCO Manufacturing Corp. Research Labs 2385 Revere Beach Parkway Everett 49, Massachusetts
	Western Development Division Headquarters P. O. Box 262 Inglewood, California
12	Attn: WDSIT
	AVCO Manufacturing Corp. Advanced Development Division 155 Sniffins Lane Stratford, Connecticut
2	Attn: Mr. J. Kerr
	Lockheed Aircraft Corporation P. O. Box 2121 Van Nuys, California
2	Attn: Dr. L. Larmore
	General Electric Company Special Defense Projects Dept. 3198 Chestnut Street Philadelphia, Pennsylvania
2	Attn: Mr. John Powers
	Rosemount Aeronautical Laboratories University of Minnesota Rosemount, Minnesota
1	Attn: Prof. R. Hermann

No. of Copies	
	Ames Aeronautical Laboratory Moffett Field, California
1	Attn: Dr. J. R. Stalder
1	Attn: Dr. M. W. Rubesin
1	Dr. Gordon N. Patterson Institute of Aerophysics University of Toronto Toronto, Canada
	Boeing Airplane Company Seattle Division Box 3707 Seattle, Washington
1	Attn: J. H. Russel, Chief Wind Tunnel Engineer
	Jet Propulsion Laboratory CIT 4800 Oak Grove Drive Pasadena, California
1	Attn: Dr. P. P. Wegener
1	Attn: Mr. L. Lees
	Polytechnic Institute of Brooklyn 527 Atlantic Avenue Freeport, New York
1	Attn: Dr. A. Ferri
	Brown University Div. of Engr. Providence, Rhode Island
1	Attn: Prof. R. F. Probstein
	University of Minnesota Minneapolis 14, Minnesota
1	Attn: Dr. E. R. G. Eckert
	Holloman Air Force Base Alamagordo, New Mexico
1	Attn: Dr. G. R. Eber
	North American Aviation Inc. Aerophysics Laboratory Downing, California
1	Attn: Dr. E. R. Van Driest

No. of Copies		No. of Copies
	U. S. Air Force Main Navy Building, Room 3816 Washington 25, D. C.	
1	Attn: Major H. W. Keller	
	Applied Physics Laboratory The Johns Hopkins University 8621 Georgia Avenue Silver Spring, Maryland	
1	Attn: Dr. F. K. Hill	
	Chance-Vought Aircraft Development Section Dallas, Texas	
1	Attn: Dr. R. E. Wilson	
	Dept. of Aeronautical Engr. Rensselaer Polytechnic Institute Troy, New York	
1	Attn: Prof. Ting-Yi Li	
	CONVAIR A Division of General Dynamics Corp. Scientific Research Laboratory 3595 Frontier Street San Diego, California	
1	Attn: Mr. M. Sibulkin	
	NOL Corona, California	
1	Attn: Code V	

Naval Ordnance Laboratory, White Oak, Md. (NAVORD report 4259)
HEAT-TRANSFER CHARACTERISTICS OF A HEMISPHERE-CYLINDER AT HYPERSONIC MACH NUMBERS, by E.M. Winkler and J.E. Danberg. 11 April 1957. 20p. illus., charts, tables, diagrs. (Aeroballistic research report 336). Projects NOL-133-1-56, and NOL-291.

UNCLASSIFIED

The heat-transfer characteristics of the laminar compressible boundary layer on a hemisphere-cylinder have been investigated at free-stream Mach numbers from 5 to 8, model wall to stagnation temperature ratios from 0.43 to 0.75, and Reynolds numbers based on body diameter from 70,000 to 700,000. Over the hemisphere, the local non-dimensional heat-transfer parameter, evaluated from the temperature differences measured across the model wall under steady-state conditions, was found to be approximately 20 percent larger than predicted for an isothermal body by Korobkin's modified incompressible theory.

1. Heat - Transference
2. Boundary layer, Compressible
3. Boundary layer, Laminar
4. Cylinders - Boundary layer
5. Cylinders - Heat transfer
6. Mach number
7. Reynolds number

I. Title
II. Winkler, E.M.
III. Danberg, J.E., jt. author
IV. Series
V. Series
VI. Project
VII. Project

Naval Ordnance Laboratory, White Oak, Md. (NAVORD report 4259)
HEAT-TRANSFER CHARACTERISTICS OF A HEMISPHERE-CYLINDER AT HYPERSONIC MACH NUMBERS, by E.M. Winkler and J.E. Danberg. 11 April 1957. 20p. illus., charts, tables, diagrs. (Aeroballistic research report 336). Projects NOL-133-1-56, and NOL-291.

UNCLASSIFIED

The heat-transfer characteristics of the laminar compressible boundary layer on a hemisphere-cylinder have been investigated at free-stream Mach numbers from 5 to 8, model wall to stagnation temperature ratios from 0.43 to 0.75, and Reynolds numbers based on body diameter from 70,000 to 700,000. Over the hemisphere, the local non-dimensional heat-transfer parameter, evaluated from the temperature differences measured across the model wall under steady-state conditions, was found to be approximately 20 percent larger than predicted for an isothermal body by Korobkin's modified incompressible theory.

1. Heat - Transference
2. Boundary layer, Compressible
3. Boundary layer, Laminar
4. Cylinders - Boundary layer
5. Cylinders - Heat transfer
6. Mach number
7. Reynolds number

I. Title
II. Winkler, E.M.
III. Danberg, J.E., jt. author
IV. Series
V. Series
VI. Project
VII. Project

Naval Ordnance Laboratory, White Oak, Md. (NAVORD report 4259)
HEAT-TRANSFER CHARACTERISTICS OF A HEMISPHERE-CYLINDER AT HYPERSONIC MACH NUMBERS, by E.M. Winkler and J.E. Danberg. 11 April 1957. 20p. illus., charts, tables, diagrs. (Aeroballistic research report 336). Projects NOL-133-1-56, and NOL-291.

UNCLASSIFIED

The heat-transfer characteristics of the laminar compressible boundary layer on a hemisphere-cylinder have been investigated at free-stream Mach numbers from 5 to 8, model wall to stagnation temperature ratios from 0.43 to 0.75, and Reynolds numbers based on body diameter from 70,000 to 700,000. Over the hemisphere, the local non-dimensional heat-transfer parameter, evaluated from the temperature differences measured across the model wall under steady-state conditions, was found to be approximately 20 percent larger than predicted for an isothermal body by Korobkin's modified incompressible theory.

1. Heat - Transference
2. Boundary layer, Compressible
3. Boundary layer, Laminar
4. Cylinders - Boundary layer
5. Cylinders - Heat transfer
6. Mach number
7. Reynolds number
I. Title
II. Winkler, E.M.
III. Danberg, J.E., jt. author
IV. Series
V. Series
VI. Project
VII. Project

Naval Ordnance Laboratory, White Oak, Md. (NAVORD report 4259)
HEAT-TRANSFER CHARACTERISTICS OF A HEMISPHERE-CYLINDER AT HYPERSONIC MACH NUMBERS, by E.M. Winkler and J.E. Danberg. 11 April 1957. 20p. illus., charts, tables, diagrs. (Aeroballistic research report 336). Projects NOL-133-1-56, and NOL-291.

UNCLASSIFIED

The heat-transfer characteristics of the laminar compressible boundary layer on a hemisphere-cylinder have been investigated at free-stream Mach numbers from 5 to 8, model wall to stagnation temperature ratios from 0.43 to 0.75, and Reynolds numbers based on body diameter from 70,000 to 700,000. Over the hemisphere, the local non-dimensional heat-transfer parameter, evaluated from the temperature differences measured across the model wall under steady-state conditions, was found to be approximately 20 percent larger than predicted for an isothermal body by Korobkin's modified incompressible theory.

1. Heat - Transference
2. Boundary layer, Compressible
3. Boundary layer, Laminar
4. Cylinders - Boundary layer
5. Cylinders - Heat transfer
6. Mach number
7. Reynolds number
I. Title
II. Winkler, E.M.
III. Danberg, J.E., jt. author
IV. Series
V. Series
VI. Project
VII. Project